

Drivers and impacts of Eastern African rainfall variability

Article

Accepted Version

Palmer, P. I., Wainwright, C. M. ORCID: <https://orcid.org/0000-0002-7311-7846>, Dong, B., Maidment, R. I. ORCID: <https://orcid.org/0000-0003-2054-3259>, Wheeler, K. G., Gedney, N., Hickman, J. E., Madani, N., Folwell, S. S., Abdo, G., Allan, R. P. ORCID: <https://orcid.org/0000-0003-0264-9447>, Black, E. C. L. ORCID: <https://orcid.org/0000-0003-1344-6186>, Feng, L., Gudoshava, M., Haines, K. ORCID: <https://orcid.org/0000-0003-2768-2374>, Huntingford, C., Kilavi, M., Lunt, M. F., Shaaban, A. and Turner, A. G. ORCID: <https://orcid.org/0000-0002-0642-6876> (2023) Drivers and impacts of Eastern African rainfall variability. *Nature Reviews Earth & Environment*, 4. pp. 254-270. ISSN 2662-138X doi: <https://doi.org/10.1038/s43017-023-00397-x> Available at <https://centaur.reading.ac.uk/110392/>

It is advisable to refer to the publisher's version if you intend to cite from the work. See [Guidance on citing](#).

To link to this article DOI: <http://dx.doi.org/10.1038/s43017-023-00397-x>

Publisher: Nature

including copyright law. Copyright and IPR is retained by the creators or other copyright holders. Terms and conditions for use of this material are defined in the [End User Agreement](#).

www.reading.ac.uk/centaur

CentAUR

Central Archive at the University of Reading

Reading's research outputs online

***Nature Reviews* referee guidelines**

Review articles

Nature Reviews publishes timely, authoritative articles that are of broad interest and exceptional quality. Thank you for taking the time to help us to ensure that our articles meet these high standards.

Review articles in *Nature Reviews* journals provide accessible, authoritative and balanced overviews of a field or topic. These articles are targeted towards readers from advanced undergraduate level and upwards, including researchers, academics and clinicians, and should be accessible to readers working in any discipline.

Please submit your report in narrative form and provide detailed justifications for all statements. Confidential comments to the editor are welcome, but it is helpful if the main points are stated in the comments for transmission to the authors.

Please note that all *Nature Reviews* articles will be thoroughly edited before publication and all figures will be redrawn by our in-house art editors. We therefore request that you concentrate on the scientific content of the article, rather than any minor errors in language or grammar.

Please consider and comment on the following points when reviewing this manuscript:

- Is the article timely and does it provide a useful addition to the existing literature?
- Are the scope and aims of the article clear?
- Are the ideas logically presented and discussed?
- Is the article accessible to a wide audience, including readers who are not specialists in your own field?
- Does the article provide a balanced overview of the literature? Please bear in mind that it may not be possible to cover all aspects of a field within such a concise article.
- Does the article provide new insight into recent advances?
- Is the discussion fair and accurate? Although our authors are encouraged to be opinionated, they should not ignore alternative points of view.
- Do the figures, boxes and tables provide clear and accurate information? Are there any additional or alternative display items that you think that the authors should include?
- Are the references appropriate and up-to-date? Do they reflect the scope of the article?
- Are you aware of any undeclared conflicts of interest that might affect the balance, or perceived balance, of the article?

Physical drivers and multifarious impacts of Eastern African rainfall variations

Paul I. Palmer^{1,2†}, Caroline M. Wainwright³, Bo Dong^{4,5}, Ross I. Maidment⁴, Kevin G. Wheeler⁶, Nicola Gedney⁷, Jonathan E. Hickman^{8,9}, Nima Madani^{10,11}, Sonja S. Folwell¹², Gamal Abdo¹³, Richard P. Allan^{4,5}, Emily C. L. Black⁴, Liang Feng^{1,2}, Masilin Gudoshava¹⁴, Keith Haines^{4,5}, Chris Huntingford¹², Mary Kilavi¹⁵, Mark F. Lunt¹, Ahmed Shaaban^{16,17} and Andrew G. Turner⁴

1) School of GeoSciences, University of Edinburgh, Edinburgh, UK;

2) National Centre for Earth Observation, University of Edinburgh, Edinburgh, UK;

3) Grantham Institute, Imperial College London, London, UK;

4) Department of Meteorology, University of Reading, Reading, UK;

5) National Centre for Earth Observation, University of Reading, UK

6) The Environmental Change Institute, University of Oxford, Oxford, UK;

7) Met Office Hadley Centre, Joint Centre for Hydrometeorological Research, Wallingford, UK;

8) Center for Climate Systems Research, Columbia Climate School, Columbia University, New York, NY, USA;

9) NASA Goddard Institute for Space Studies, New York, NY, USA;

10) UCLA Joint Institute for Regional Earth System Science and Engineering, CA, USA;

11) Jet Propulsion Laboratory, Pasadena, CA, USA;

12) UK Centre for Ecology and Hydrology, Wallingford, UK;

13) Department of Civil Engineering, University of Khartoum, Khartoum, Sudan;

14) IGAD Climate Prediction and Applications Centre, Nairobi, Kenya;

15) Kenya Meteorological Department, Nairobi, Kenya;

16) Department of Atmospheric and Environmental Sciences, University at Albany, State University of New York (SUNY), Albany, NY, USA;

17) Egyptian Meteorological Authority, Cairo, Egypt.

† email: paul.palmer@ed.ac.uk

Abstract

Eastern Africa experiences extreme rainfall variations that have profound socio-economic impacts. In this Review, we synthesize understanding of observed changes in seasonal regional rainfall, its global to local forcings, the expected future changes and the associated environmental impacts. We focus on regions where annual bimodal rainfall is split between long rains (March-May) and short rains (October-December). Since the early 1980s, the long rains have got drier although some recovery is observed in 2018 and 2020 (-0.12—1.23 mm/season/decade). Meanwhile, the short rains have got wetter (1.27—2.58 mm/season/decade). These trends, overlaid by substantial year-to-year variations, impact the severity and frequency of extreme flooding and droughts, the stability of food and energy systems, the susceptibility to water-borne and vector-borne diseases and ecosystem stability. Climate model projections of rainfall changes vary but there is some consensus that a warming climate will increase rainfall over Eastern Africa. They suggest that by 2030-2040 the short rains will deliver more rainfall than the long rains, which has implications for sustaining agricultural yields and triggering climate-related public health emergencies. Mitigating the impacts of future Eastern African climate requires continued investments in agriculture, clean water, medical and emergency infrastructures that are commensurate to the upcoming existential challenges.

49
50
51
52
53
54
55
56
57
58
59
60
61
62
63
64
65
66
67
68
69
70

Key points [30 words or fewer]

- Rainfall across Eastern Africa is changing rapidly with future projections suggesting these changes will continue, driven by increasing atmospheric greenhouse gases and by intrinsic natural variability of the climate system.
- Within the 2030-2040 timeframe, subject to caveats, climate models suggest that the short rains will deliver more rainfall over Eastern Africa than the long rains that has traditionally supported agriculture.
- During the same period, climate models suggest a higher frequency of droughts that are also associated with significant humanitarian and socio-economic impacts.
- Projected rainfall changes will lead to widespread changes in agricultural yields and accessibility to clean water that will further increase the risk of food and water insecurity across Eastern Africa.
- More broadly, future rainfall changes will result in multifarious and long-term costs to human health and wellbeing, and the urban and natural environments.
- Development of adaptation strategies to improve agricultural yields and access to clean water, and to prepare for vector-borne disease outbreaks will help avoid an unprecedented-scale public health emergency.
- Targeted improvements to meteorological observing systems will help improve the quality of meteorological forecasts over Eastern Africa that enable early warning systems to deliver better actionable information to individual countries

71
72

Introduction

73
74
75
76
77
78
79
80
81
82
83
84
85
86
87
88
89
90
91
92
93
94
95

Seasonal rainfall is integral to the 457 million people living across Eastern Africa, a region including Somalia, Burundi, Djibouti, Ethiopia, Eritrea, Kenya, Rwanda, South Sudan, Sudan, Tanzania and Uganda (**Box 1**). The number, duration and timing of these seasons varies across the region, driven principally by the movement of the intertropical convergence zone (ITCZ)¹. For instance, the most northern and southern countries (northern Ethiopia, Eritrea, Sudan, South Sudan and southern Tanzania) experience a single summer wet season for their respective hemisphere. In contrast, countries between these latitudinal extremes (encompassing Kenya, Uganda, Somalia, Burundi, Rwanda and parts of northern Tanzania and southern Ethiopia) experience two wet seasons. These two wet seasons occur during boreal spring (typically March-May, MAM; the more intense long rains) and autumn (typically October-December, OND; the less intense short rains), although there are substantial regional variations in these timings. We focus mainly on countries that have annual bimodal rainfall.

This seasonal rainfall is vital to the health and economic prosperity of the region. For example, long rains support agricultural production and thus national food security. Rain-fed agriculture, in turn, has a substantial role in the economy of many Eastern African countries. Agriculture employs 67% of people in Ethiopia, 80% in Somalia, 54% in Kenya, 63% in Eritrea, 38% in Sudan and 21% in Egypt (data taken from World Bank Open Data). Agriculture also represents a substantial contribution to the annual multi-billion-dollar export of goods such as sugar, tea, coffee, tobacco, nuts and seeds, cut flowers and vegetables (taken from the Observatory of Economic Complexity). Moreover, rainfall is pivotal to energy production, particularly given that hydropower represents a substantial fraction of electricity generation in Eastern Africa².

96 Aquifer recharge from rainfall³ also provides a sustainable reservoir of groundwater for potable
97 water (and irrigation) during periods of drought³, demonstrating the importance of rainfall for
98 water security, especially when looking to the future⁴.

99
100 Observed rainfall variability, particularly the disruption to the long and short rains, can
101 therefore result in a wide range of humanitarian, economic and environmental impacts. For
102 example, three anomalously low rain seasons over Somalia from April 2016 to December
103 2017 resulted in sustained and widespread drought conditions that led to significant losses of
104 agricultural crops and livestock⁵. Consequently, more than six million people faced acute food
105 shortages and malnutrition⁶, exacerbated by a shortage of potable water that led to disease
106 outbreak. A similar situation is unfolding in 2022 (ref ⁷), with poor rain seasons since late 2020.
107 In stark contrast, consecutive anomalously high rain seasons over South Sudan since 2019
108 has led to prolonged flooding, affecting more than 800,000 people⁸. Recurrent flooding has
109 damaged water treatment facilities, leaving millions without potable water, resulting in the
110 outbreak of cholera and diseases spread by mosquitoes. Fields that typically support
111 subsistence farming are submerged by floodwater, leading to a significant reduction in land to
112 cultivate. This situation is exacerbated by conflict⁸. As such, there are concerns over
113 widespread disruptions to clean sources of energy², depletion of surface and groundwater
114 reservoirs⁹, devastating flooding events¹⁰, and reductions in agricultural crop yields¹¹ and
115 livestock productivity¹². To help mitigate such impacts and inform future adaptation changes,
116 it is therefore vital to fully understand all aspects of East African rainfall impacts, particularly
117 in light of continued changes arising from anthropogenic warming¹³.

118
119 In this Review, we synthesize the literature regarding observed rainfall variations over Eastern
120 Africa, focused on regions with a bimodal rainfall season, and their physical drivers. We
121 subsequently outline the economic, humanitarian and environmental impacts of such
122 observed rainfall variability. Based on state-of-the-art climate model projections, we also
123 describe the major climatological changes anticipated for Eastern Africa, and the associated
124 likely future impacts. Finally, we identify key gaps in knowledge and how these can be
125 addressed in future research.

126 127 **2 Drivers of Eastern African rainfall**

128
129 The timing and magnitude of the seasonal cycle of rainfall varies across Eastern Africa (**Fig.**
130 **1**). A single peaked seasonal cycle is evident over the broader Nile basin during JJA, whereas
131 two distinct rainfall seasons (short rains and long rains) are observed over the Juba-Shabelle
132 and northeast coast basins; some combination of the two occur over the Rift Valley basin and
133 the central-East coast basin.

134
135 There are substantial seasonal and interannual variations in rainfall totals (**Fig. 1**). For
136 example, the standard deviation of rainfall over the Nile Basin during August (typically the
137 wettest month) is 17mm month⁻¹, representing ~12% of the long-term August mean rainfall
138 according to the GPCP dataset. Whereas across the Juba-Shabelle Basin, rainfall is
139 considerably more variable. The standard deviation is 36 mm month⁻¹ during the peak of the
140 long-rains (April) and 52 mm month⁻¹ during the peak of the short-rains (October), representing
141 30% and 60% of their long-term means, respectively. The variability over the Juba-Shabelle
142 Basin during October is such that extremes between 1983-2019 have been recorded with a
143 minimum of just 34 mm month⁻¹ in 2003 (39% of the long-term mean) and a maximum of 305

144 mm month⁻¹ in 1997 (355% of the long-term mean). This variability is driven by various local
145 and remote physical processes, which we now discuss.

146

147 **2.1. Global teleconnections**

148 Rainfall variability over Eastern Africa is influenced by a range of global and regional modes
149 of climate variability (**Fig. 2**), including the El Niño Southern Oscillation (ENSO), the Indian
150 Ocean Dipole (IOD), the Quasi-Biennial Oscillation (QBO) and the Madden-Julian Oscillation
151 (MJO).

152 The IOD is a key driver of variability across Eastern Africa during the short rains. The positive
153 phase of the IOD is defined by sustained positive SST anomalies in the western Indian Ocean
154 (50°E-70°E, 10°S-10°N) and negative SST anomalies in the eastern Indian Ocean (90°E-
155 110°E, 10°S-0°S), resulting in an SST difference between the two that exceeds +0.4°C. The
156 positive IOD is linked with wetter short rains over Eastern Africa (**Fig. 2**), with precipitation
157 totals that can be 2-3 times the long-term mean¹⁴, as seen in 1997, 2006, 2012, 2015 and
158 2019. The negative IOD, defined by a sustained SST difference <-0.4°C, is associated with
159 weaker short rains¹⁵, resulting in 20-60% of the long-term mean rainfall.

160 Links between ENSO and Eastern African short rains are also apparent¹⁶. East Pacific and
161 central Pacific El Niño events typically result in wetter short rains over Eastern Africa, and La
162 Niña conditions result in drier short rains¹⁷ (**Fig. 2**). However, the ENSO impact on Eastern
163 Africa is strongly mediated by the IOD¹⁶. The typical concurrence of positive IOD with East
164 Pacific El Niño, and negative IOD with East Pacific La Niña, act to amplify precipitation
165 responses, resulting in even larger anomalies across the region. For instance, the
166 coincidence of the 1997 El Niño with a strong positive IOD event led to rainfall anomalies of
167 200% above climatological mean values over the short rains season¹⁴. In contrast, the strong
168 central Pacific El Niño of 2015 coincided with a weaker IOD, producing anomalies ~50% above
169 the climatological mean¹⁶. However, these relationships are non-linear, as demonstrated by
170 extreme 2019/2020 rainfall that occurred during an anomalously positive phase of the IOD but
171 neutral ENSO conditions¹⁸.

172 The IOD and ENSO physically influence East African rainfall by modifying the Indian Ocean
173 Walker Circulation (**Fig. 2**). In the absence of a strong phase of ENSO and IOD during the
174 rainy season, the Indian Ocean Walker Circulation consists of a strong upward branch over
175 the western Pacific warm pool and a much weaker updraft over Eastern Africa. However, when
176 there are unusually warm SSTs over the western Indian Ocean and central Pacific and
177 unusually cool SSTs over Southeast Asia (a positive IOD and El Niño conditions), the Indian
178 Ocean Walker Circulation weakens^{19,20}; a strong branch of rising air occurs over the western
179 Indian Ocean and a strong branch of sinking air over the western Pacific. This circulation
180 pattern is associated with elevated rainfall over Eastern Africa. A concurrent positive IOD and
181 El Niño event reinforces these impacts, leading to enhanced rainfall anomalies during short
182 rains over Eastern Africa¹⁶.

183 Strong El Niño events can lead to warmer SSTs in the Western Pacific (sometimes referred
184 to as a “Western V Pattern”²¹). Warmer SSTs in the western equatorial Pacific are linked to
185 drier short rains over Eastern Africa and warmer SSTs in the western North Pacific are

186 associated with dry conditions during the long rains. Warmer SSTs over the western North
187 Pacific strengthen the Walker Circulation that suppresses Eastern African long rains. This SST
188 pattern led to successive dry seasons and droughts across Eastern Africa during 2016-2017
189 (ref²¹). Variations in the long rains are less sensitive to changes in IOD²², since the IOD peaks
190 several months later (during September-November) than the peak long rains.

191
192 The pan-tropical MJO is a further driver of sub-seasonal rainfall variability over Eastern Africa,
193 influencing both the long and short rains on a monthly basis²³. The MJO is described in terms
194 of eight phases, corresponding to locations of elevated convection (and rainfall). For example,
195 MJO phases 2-4 are linked with large-scale convection in the Indian Ocean, resulting in
196 westerly wind anomalies and enhanced rainfall¹⁶ (including 22%-78% of extreme rainfall
197 events, depending of MJO phase and amplitude²⁴) over the Eastern African highlands²⁴⁻²⁶
198 (**Box 1**). This relationship is weaker in October and April than in November, December, March
199 and May²⁷. In contrast, MJO phases 6-8 are associated with suppressed convection across
200 Eastern Africa and the western Indian Ocean, but wet conditions over low-lying coastal
201 regions^{24,25}. Greater seasonal rainfall accumulations are observed during a long rains season
202 when the MJO is more active in any phase²⁸, with the MJO explaining ~20% of the observed
203 interannual rainfall variations.

204
205 Through its relationship with the MJO²⁹, the eastward phase of the QBO also influences
206 Eastern African rainfall. Above average long rains are linked to an easterly QBO in the
207 preceding September-November²⁸. This 6-month lag³⁰, is consistent with the time scale
208 associated with the descent of mid-stratospheric wind anomalies to the tropopause³¹. The
209 QBO typically explains <20% of observed interannual rainfall variations, and the strength of
210 this lagged correlation is dependent on which model reanalysis product is used³², due to
211 model-specific assumptions about convective parameterizations.

212 213 **2.3. Local drivers of variability**

214 Variations in Indian Ocean SSTs, particularly those in the west that are partially controlled by
215 the IOD²⁸, are also linked with variability in both rainy seasons. Warmer SSTs heat the
216 boundary layer leading to anomalous ascent, opposing the climatological subsidence and
217 corresponding drying, thereby enhancing rainfall. Positive SST anomalies in the western
218 Indian Ocean increase the magnitude of short rains over 95% of equatorial East Africa³³, and
219 explain 9-26% of observed rainfall variations during the long rains²⁸. The positive correlation
220 between western Indian Ocean SSTs and rainfall is strongest at the beginning and end of the
221 long rains season³⁴ when the rainfall is less well established and more susceptible to local and
222 remote forcing. Rainfall during the peak of the long rains (April) is also significantly correlated
223 with southern Atlantic SSTs, whereby cooler SSTs lead to higher rain rates over Kenya via
224 zonal winds over central Africa³⁴.

225 The presence of tropical cyclones in the southwest Indian Ocean (when MJO is in phases 3-
226 4) is associated with low-level westerly flow over Eastern Africa, resulting in enhanced
227 rainfall³⁵. There is a greater likelihood of westerly flow when the cyclones are located to the
228 east of Madagascar²⁶. The cyclone locations and rainfall impacts over Eastern Africa in 2018
229 and 2019 are consistent with this west/east pattern^{35,36}. Cyclones Dumazile and Eliakim in
230 2018 were located east of Madagascar and were associated with westerly flow and enhanced

231 rainfall, while Cyclone Idai in 2019 was located west of Madagascar and coincided with a drier
232 period^{35,36}.

233 The influence of the Congo airmass, characterized by the 700hPa zonal winds, has also been
234 associated with interannual variability of the long rains^{26,34}. Despite climatological easterly
235 winds, westerly winds originating from the Congo sometimes occur during March-May (often
236 linked to phase 3-4 of the MJO²⁶), bringing moist air that leads to convergence around Lake
237 Victoria and enhances rainfall^{26,34}. Indeed, the cumulative rainfall total of the long rains is
238 further strongly correlated with 700hPa zonal winds across the Congo Basin and Gulf of
239 Guinea. In contrast, enhanced surface westerlies from the Congo basin, driven by a higher
240 geopotential height gradient over the Congo Basin than the western Indian Ocean, lead to
241 wetter long rains over Tanzania³⁷.

242 **3 Observed changes in Eastern African rainfall**

243
244 In addition to interannual variability driven by remote and local drivers, precipitation across
245 Eastern Africa also exhibits decadal-scale trends. Since the early 1980s, a range of satellite-
246 derived rainfall data products have helped to quantify these changes^{38,39} (**Fig. 3**). These data
247 products show consistent wetting trends over the Ethiopian highlands (-5—12°N, 34—38°E)
248 during March-May (long rains) and the Horn of Africa (-2—12°N, -35—51°E) during October-
249 December (short rains), with ranges across different datasets of 0.7-1.7 mm/season/yr and
250 1.6-3.4 mm/season/yr, respectively (**Fig. 3a, b**). Elsewhere in Eastern Africa, however, rainfall
251 trends based on satellite data are inconsistent in magnitude and sign during both rainy
252 seasons, with the largest discrepancies between data products over the eastern Congo Basin
253 (**Fig. 3a, b**).

254
255 In addition to discrepancies between satellite datasets, substantial differences between
256 satellite products and gauge-based records over Eastern Africa add to the uncertainty in
257 estimating long-term spatially resolved seasonal rainfall trends (**Fig. 3c, d**). For example, while
258 satellite records reveal statistically significant trends, gauge-based records from the 1950s to
259 2018 do not display significant trends in precipitation or streamflow⁴⁰. These differences arise
260 from contrasting satellite rainfall estimation methodologies, and spatial and temporal gaps in
261 the rain gauge network^{41,42}. However, there is better agreement between areal-weighted
262 rainfall means from different data products in both rainy seasons (**Fig. 3c, d**), particularly after
263 year 2000 when there are fewer gaps in the satellite records⁴³, resulting in greater confidence
264 in reported rainfall trends for both the long and short rains.

265 266 **3.1. Long rains**

267 Over Eastern Africa, consistent negative long rain trends were observed over 1985-2010. The
268 magnitude of these trends is sensitive to the dataset used, ranging from -14mm yr⁻¹ to -65mm
269 yr⁻¹ per decade (**Fig. 3a, c**). Particularly marked declines occurred in ~1999 and 2010-2011
270 (refs ⁴⁴⁻⁴⁷), the latter event causing devastating droughts in Kenya, Somalia and south-eastern
271 Ethiopia. Trends calculated up until ~2017 also continue to be negative. However, very wet
272 long-rains in 2018 and 2020 indicate some recovery (**Figure 3a, c**). Trends computed between
273 1983-2021 therefore no longer indicate widespread and consistent drying across the Horn of
274 Africa. Instead, less consistency emerges among datasets (**Fig. 3a, c**), with some indicating

275 a general wetting trend (TAMSAT, 1.23 mm season⁻¹ yr⁻¹; 0.47% season⁻¹ yr⁻¹) and others an
276 overall drying trend (GPCC, -0.13 mm season⁻¹ yr⁻¹; -0.08% season⁻¹ yr⁻¹).

277 Different mechanisms have been proposed to explain this reduction in the long rains up to the
278 2000s. On the one hand, the decline has been linked to Pacific Ocean SST variability^{48–50}.

279 Specifically, Pacific Decadal Variability manifests as a pattern of SST that has a larger
280 latitudinal extent than associated with ENSO, and has been described as a “Western V”
281 pattern that encapsulates warm SST values centred over the western Pacific warm pool with
282 tongues of warm SSTs extending northeastward toward Hawaii and southeastward into the
283 southern central Pacific^{21,51}. Warming of Indo-Western Pacific SSTs enhances convection
284 over the western equatorial Pacific leading to an anomalous Walker circulation over the Indian
285 Ocean, strengthening of the upper-level easterlies, increased subsidence over East Africa in
286 the descending branch, and consequently reduced rainfall during the long rains^{52,53}. In some
287 instances, the strengthening of the upper-level easterlies has been highlighted as the
288 dominant driver in this process, with minimal connections to Walker Circulation variability⁵³.
289 More rapid warming of the West Pacific relative to the East Pacific since 1998, associated with
290 a negative phase of the Pacific Decadal Oscillation⁵⁴, has been linked with a greater
291 susceptibility of the long rains to drought during La Niña events with an increased risk of
292 concurrent short-long rains droughts²¹. Strengthening of the W-E SST gradient across the
293 Pacific since 1998 has led to a stronger Walker circulation and faster Pacific trade winds^{55,56}
294 that results in drying over Eastern Africa via Indian Ocean teleconnection, in contrast with
295 coupled climate model runs⁵⁷.

296 On the other hand, the shortening of the long rains season⁴⁵ (later onset and earlier cessation)
297 from the 1980s to late 2000s has been attributed to the rainfall decline. In this case, faster
298 SST warming in the Arabian Sea compared to further south, enhances pressure the gradient
299 and thus a faster-moving rainband. Declining westerly 700 hPa winds are also linked with the
300 decadal drying trend during the long rains⁴⁶, driven by changes in geopotential height gradient
301 that are associated with increased heating around Arabia and the Sahara⁴⁶. Positive
302 anomalies in westerly winds are associated with enhanced rainfall over East Africa (section
303 2.3) and conversely declining westerlies are associated with reduced rainfall. Finally, internal
304 variability^{45,46} such as variations in SST that are not linked with radiative forcing, is also thought
305 to be a driver.

306 **3.2 Short rains**

307 Compared to the long rains, there is greater consistency in the sign and magnitude of short
308 rain trends (**Fig. 4b, d**). Trends calculated over 1983-2021 are broadly consistent across
309 CHIRPS and TAMSAT, each highlighting an increase in short rain totals of 50-100 mm. We
310 do not report the trend for GPCC because it is not available beyond 2019 but it is consistent
311 with CHIRPS and TAMSAT for the shorter period of 1983-2019. We also do not report the
312 trend for ARC because it includes spurious time-varying jumps⁴¹ that compromise a robust
313 estimate for the trend. Spatially, all datasets exhibit this increasing rainfall trend over large
314 parts of Tanzania, Uganda, Kenya, Somalia and Ethiopia (**Fig. 4b**), ranging 1.27—2.58 mm
315 season⁻¹ yr⁻¹ (0.92—1.82% season⁻¹ yr⁻¹).

316
317 As with the long rains, regional-mean long-term linear trends in short rains rainfall are
318 punctuated with periods of anomalous rainfall. For example, short rain totals during 1997-1998

319 and 2019-2020 were 2-3 times higher than climatological values¹⁴, the former being linked to
320 the El Nino event^{47,58} and corresponding connections to the positive IOD, with the largest
321 positive rainfall anomalies of 100-250 mm yr⁻¹ reported in 1997, 2006, 2012, 2015, and 2019
322 (**Fig. 4d**). This is consistent with earlier analyses^{49,50} and with mechanisms that determine
323 year to year variations.

324
325 We find that including 2020 and 2021 does not change the spatial pattern of rainfall changes
326 during OND but does increase the magnitude of the wetting trend in the short rains, as it does
327 for the long rains. In general, we find that the regional-mean wetting trend is mostly a result of
328 short-term variability driven by changes in ENSO and the IOD.

329 **3.3 Anthropogenic connections**

330
331 Large year-to-year variability in the long and short rains discussed in the previous section
332 present a difficulty in interpreting drivers and isolating the anthropogenic imprint. Paleoclimate
333 reconstructions provide a longer-term view of rainfall changes over Eastern Africa. They show
334 that changes in rainfall in the last century across the globe are not unprecedented in the
335 context of the past two millennia, but the rate at which rainfall is changing is unusual. These
336 data reveal a drying trend over the past two centuries⁴⁸ and a recent increase in drought
337 frequency over the Horn of Africa during March-May⁵⁹.

338
339 Greenhouse gas-induced warming drives an increase in atmospheric moisture and its
340 convergence which intensify wet seasons while higher temperatures and greater evaporative
341 demand intensify dry seasons, contributing to a greater severity of wet and dry extremes⁶⁰.
342 Cooling from anthropogenic aerosols have offset these greenhouse gas changes, and,
343 through an additional altered global distribution of aerosol forcing, have been implicated in a
344 southward shift in the African ITCZ from the 1950s to the 1980s (ref ⁶¹). Recovery from this
345 altered state has been attributed to a combination of greenhouse gas and aerosol forcing⁶².
346 While there is some consensus about the human influence on rainfall over Eastern Africa (via
347 greenhouse gas induced warming and cooling from anthropogenic aerosols^{19,62,63}), the
348 anthropogenic influence on the physical processes (specifically the IOD) that control year-to-
349 year rainfall changes is less clear^{53,64}. Based on a combined model and data analysis, drought
350 trends over Eastern Africa are most consistent with changes in precipitation rather than
351 increasing temperature⁶⁵.

352
353 An increased frequency of the positive phase of the IOD during the second half of the twentieth
354 century has not led to higher seasonal rainfall amounts compared to the first half of the
355 twentieth century⁵³. This observation is consistent with understanding of how a warming
356 climate perturbs the thermal structure of the atmosphere and the circulation of the tropical
357 oceans^{66,67}, resulting in a long-term weakening of Walker and Hadley circulations and the
358 narrowing of the ITCZ^{53,68,69}. Yet, observed strengthening of the Walker circulation since the
359 1990s, associated with rapid warming of the tropical west Pacific relative to the east Pacific,
360 is not reproduced well by simulations and this has been linked with systematic model biases
361 that may limit the projections of Eastern African rainfall⁶⁷. Therefore, anthropogenic signals of
362 Eastern Africa rainfall are yet to be clearly established in the observational record and future
363 projections assessed in Section 5 should be interpreted in the context of these complex
364 present-day drivers and uncertainties.

4 Impacts of observed rainfall variations

Local and remotely driven variability in the short and long rains have substantial and multifarious environmental, humanitarian and economic impacts occurring over various temporal scales. Given the diversity of the impacts of Eastern African rainfall variability, we focus here on three broad groupings: agriculture, natural ecosystems, and water security. These impacts are not exhaustive but represent a diverse subset of widely researched topics. It is also important to bear in mind that precipitation impacts do not occur in isolation; often such impacts coincide with changes in temperature, complicating explicit attribution to rainfall.

4.1. Agricultural impacts

Rainfall variability across Eastern Africa affects agriculture directly and indirectly. Much agriculture in the region is rain-fed. As such, failure of seasonal rains result in agricultural droughts, the frequency of which has increased from once every ten years in the early 1900s to once every three years since 2005 (ref⁷⁰). While small- and large-scale irrigation schemes are helping to mitigate the impacts^{71,72}, minimal infrastructure exists to retain, redistribute and store water to cope with this intra-seasonal and interannual variability. The resulting loss of agricultural production has thus been the cause of some of the most well-known humanitarian disasters in the 20th and 21st centuries, including the 1974 Sahel drought which resulted in an estimated 325,000 deaths, and the 1984 drought across Ethiopia and Sudan that caused 450,000 deaths^{73–75}. Since then, Ethiopia has experienced several droughts. One responsible factor is El Niño, which results in contrasting impacts over Ethiopia⁷⁶: lower than normal rainfall over northern Ethiopia that responds similarly to the Sahel region, and higher than normal rainfall over southern Ethiopia that can lead to flooding. Variations in the climate system, e.g., location of the ITCZ, and regional orography (**Box 1**) complicate this relationship.

The 1997/1998 drought illustrates other clear agricultural impacts. Cereal production⁷⁷ declined by 25% during this period, resulting in price increases of 15-45%. This was due to lower crop yields due to drought and indirectly by reduced cultivated land because of malnourished oxen⁷⁸. Reduced crops also caused cattle mortality rates of 26% in some regions due to dehydration/starvation and disease⁷⁹, with cattle typically more affected by drought than camels or small ruminants⁸⁰. Production of coffee, a key export crop for the country, was also substantially reduced by heavy rain in late 1997 that stripped coffee berries from their trees⁷⁸. Efforts to implement drought early-warning systems^{81,82}, increase agricultural capacity by distributing drought-resistant seeds, and enhance rapid humanitarian responses from governments and international aid which seek (and have arguably helped) to mitigate deaths associated with food security^{83,84}. Humanitarian impacts of the historic drought⁸⁵ in 2015 and subsequent droughts⁸⁶, due to consecutive failed rain seasons in parts of Ethiopia (and elsewhere over East Africa), demonstrate the complex and evolving challenges faced by East African countries.

While below normal rainfall threatens agriculture, so does an increase in rainfall intensity. In regions that are moisture limited, benefits from increased rainfall can be expected⁸⁷. However, in regions with low permeability soils such as the clay vertisols of the sub-humid regions of Ethiopia that have infiltration capacities of only 2.5 to 6.0 cm/day, the landscape is easily overwhelmed by intensive rainfall⁸⁸. Low permeability of irrigated lands results in waterlogging and crop damage, and poor drainage systems substantially limit the production potential of

415 the soils⁸⁹. For example, productivity losses of 45% over 60 years have been recorded for
416 some Ethiopian sugar plantations due to waterlogging. Furthermore, the erosion of agricultural
417 topsoil occurs when runoff from sloped terrain exceeds the rate of soil intake⁹⁰, affecting future
418 productivity. An illustration of this is the unusually heavy rainfall over northern Ethiopia during
419 March and April 2016, immediately following extensive drought conditions, which led to
420 widespread flooding, landslides, displacement of people, and damage to crops. Based on
421 recent changes in rainfall over Eastern Africa, there is a growing influence of extreme rainfall
422 seasons that will continue to negatively impact agricultural productivity.

423

424 High densities of desert locusts (*S. gregaria*) also pose a threat to agricultural crops and are
425 strongly linked to rainfall variability. Heavy and extensive rainfall provides moist soil for egg
426 laying, and the subsequent rain-fed flushing of vegetation provides shelter and food for the
427 locusts causing widespread damage. As such, rainfall is a dominant factor governing their
428 population and movement, as evidenced by several documented locust plagues over Eastern
429 Africa^{91–94}. The extent of crop damage is related to successfully locating locusts breeding
430 grounds and to proactive interventions that are sometimes compromised by armed conflict⁹⁵.
431 Given rainfall connections to the IOD and ENSO, locust plagues and resulting crop damage
432 typically occur during positive IOD years when rainfall is enhanced⁹⁶, for example, the years
433 1986/1987, 1992/1993, and 2019/2020. These remote drivers often interact with local drivers.
434 For example, the 2020 locust outbreak—the worst in 25 years for Ethiopia and Somalia and
435 in 70 years for Kenya—has been linked to the rare landfall of two tropical cyclones in the
436 Arabian Peninsula during 2018, exponential growth in breeding through the creation of
437 ephemeral lakes, their southward migration to East Africa, and subsequent establishment of
438 the swarm from IOD-related enhanced vegetation growth. The COVID-19 pandemic along
439 with other factors prevented proactive interventions in this case and resulted in an estimated
440 US\$8.5billion in crop damage in Yemen and East Africa during 2020, amplifying threats to
441 food security. Indeed, between December 2019 and March 2020, 114,000, 41,000 and 36,000
442 hectares of sorghum, maize and wheat were estimated to be damaged, respectively.

443

444 SSTs prior to cyclogenesis have got progressively warmer over the north Indian Ocean⁹⁷ over
445 the period 1980–2020, facilitating higher heat fluxes from the ocean to the atmosphere that
446 are linked to the frequency and intensity of cyclones. Generally, differential warming of SSTs
447 across the Indian Ocean affects the location of cyclogenesis. Particularly, there has been rapid
448 warming over the Arabian Sea and the Bay of Bengal thereby increasing the chances of the
449 storms reaching land and creating ephemeral lakes that can sustain locust breeding. Indeed,
450 three times the number of cyclones affected the Arabian Peninsula during the 2010s
451 compared with the previous two decades. The frequency of cyclones in the north Indian Ocean
452 is also linked with warmer SSTs over the eastern Indian Ocean associated with the negative
453 IOD pattern⁹⁸.

454

455 **4.2 Ecosystem impacts**

456

457 Rainfall variability also has strong bearing on various ecosystem functions, including terrestrial
458 gross primary production (GPP), wildfire activity and wetland emissions of greenhouse gases.

459

460 Terrestrial GPP—the total amount of carbon fixed by plants—is closely related to water
461 availability in East Africa's tropical forest and savannah ecosystems⁹⁹. Tropical African
462 ecosystems are typically more limited by water than sunlight on a regional basis^{100,101}.

463 Interannual variations in water availability⁹⁹ through rainfall and groundwater result in GPP
464 variations within $\pm 10\%$ of climatological values. For forest ecosystems, GPP anomalies are
465 highly correlated with changes in groundwater and soil moisture, generally increasing during
466 periods of elevated rainfall, except in regions where annual rainfall exceeds 1800 mm⁹⁹. This
467 decline in productivity with higher rainfall may reflect reduced sunlight due to cloud cover. For
468 savanna ecosystems, rainfall patterns have a stronger influence on inter-annual variability in
469 productivity. Although, productivity in these ecosystems is also controlled by soil moisture and
470 groundwater because shrubs in dry savannas may still have access to below surface water¹⁰²
471 due to their deep rooting systems.

472
473 Much less is known about how African ecosystems respond to changes in rainfall than other
474 tropical ecosystems, but models of GPP driven by satellite observations of vegetative
475 properties, rainfall, and groundwater are beginning to improve our understanding. Based on a
476 GPP product¹⁰³ inferred from the NASA SMAP satellite instrument, the annual mean GPP for
477 2003-2017 is $\sim 3.08 \pm 0.19$ Pg/yr. Drought years of 2005 and 2015 and elevated rainfall in 2010
478 exemplify the range of GPP responses to rainfall changes that were driven by SST anomalies
479 in the South Atlantic and Indian Oceans. The weak El Niño year of 2005, immediately
480 preceded by years of anomalously low rainfall and depleted groundwater, led to a drop of 5%
481 in GPP over -5 - 10°N , 30 - 50°E (-0.15 Pg/yr). In contrast, in 2015 when there were similarly
482 weak El Niño conditions, anomalously low rainfall, particularly over latitudes -10 - 10°N , was
483 partially offset with groundwater reserves that were replenished in the preceding five years,
484 resulting in a GPP of 3.19 Pg/yr, close to the climatological mean value. During the strong
485 2010 El Niño, there were widespread increases in GPP across the region ($+0.15$ Pg/yr,
486 representing $+5\%$) except for parts of the Horn of Africa. Groundwater reservoirs can act as a
487 temporary buffer against drought during years of low rainfall for sufficiently deep rooting
488 systems, but only if they have an opportunity to replenish during anomalously wet years.
489 Regions that suffer from consecutive years of below average rainfall, such as countries in the
490 eastern most part of Horn of Africa, will see drops in GPP and eventually increasing rates of
491 vegetation mortality.

492
493 By influencing GPP, rainfall variability can also influence vegetation fire activity and
494 consequently emissions of air pollutants, CO_2 and other GHGs¹⁰⁴⁻¹⁰⁶. For example, above
495 average rainfall during the growing season increases plant productivity, thereby increasing the
496 fuel load available for burning in subsequent seasons or years¹⁰⁷. In contrast, above average
497 rainfall during the dry season can suppress fire activity, although fire ignition via lightning is
498 enhanced during moist convection¹⁰⁸. Both processes have proven to be important in Eastern
499 Africa during initial years of the 21st century¹⁰⁹.

500
501 Landscape fires in Eastern Africa are typically focused on South Sudan and parts of western
502 Ethiopia and northern Uganda during January, and Tanzania and part of southern Uganda
503 during July. During the 2001-2012 period, changes in rainfall explained about 20% negative
504 trends in burned area in South Sudan¹¹⁰. Based on ENSO events during 1997-2016, El Niño
505 years lead to a small reduction in burned area anomalies in forest and non-forest ecosystems
506 over northern hemispheric Africa. Generally, ENSO plays a smaller role in burned area and
507 subsequent emissions than in other tropical biomass burning regions¹¹¹. This is supported by
508 an ensemble analysis of Earth system models (ESMs)¹¹².

509

510 Tropical wetland emissions of methane exhibit marked relationships with precipitation given
511 the dominant control of inundation extent and water table depth^{113,114}. Aquatic production of
512 methane is due to anoxic decomposition of organic matter from root systems and decaying
513 plants, influenced by a range biochemical and phenological factors^{115–117} and local macrophyte
514 diversity^{118,119}.

515

516 Satellite data revealed the global significance of Eastern African wetland emissions of
517 methane over South Sudan and western Ethiopia during the long and short rain periods over
518 the last decade^{120–123}. Seasonal variations in emissions are controlled by local rainfall, whilst
519 longer-term changes are driven mostly by rainfall collected by upstream catchment areas (for
520 example, Lake Victoria, Lake Albert). Water released from these catchments is transported
521 downstream via the White Nile leading to demonstrable increases in wetland extent and
522 associated vegetation flushing, particularly over the Sudd^{124,125}. Methane emissions from the
523 Sudd in South Sudan during 2010-2016 represented about a third of global atmospheric
524 emissions. A strong positive phase of the IOD during 2018-2019 led to anomalously large
525 rainfall over Uganda and Kenya during March-May 2018 and October-December 2019,
526 equivalent to a once in 30-year event¹²⁶. The additional methane emissions from Eastern
527 Africa, focused on South Sudan and Ethiopia, during the short rains in 2019 represented a
528 quarter of the global atmospheric methane growth rate for that year¹²⁶. The anomalous global
529 atmospheric methane growth rates in 2020 (ref ^{127,128}) and 2021 (ref ¹²⁸) have also been partly
530 attributed to anomalous Eastern African wetland emissions.

531

532 Wetlands can also be hotspots of ammonia (NH₃) gas emissions^{129,130}. Ammonia is a
533 precursor to the formation of secondary inorganic aerosols, which are the main contributor to
534 particulate matter globally and represents a hazard to human health^{131,132}, and its deposition
535 to downwind ecosystems can lead to eutrophication, soil acidification, reduced productivity,
536 biodiversity decline, and indirect GHG emissions^{133–136}. Ammonia is volatilized from
537 ammonium in soils via an abiotic reaction, which is influenced by pH, temperature, and, of
538 importance here, soil moisture content linked to changes in rainfall. When soils with high
539 moisture content start to dry out, NH₃-nitrogen tends to become more concentrated at the
540 same time as there are reduced limits on gas diffusion through soils, which, along with other
541 factors, leads to enhanced NH₃ emissions^{137–139}.

542

543 These processes have been shown to produce a large seasonal increase in NH₃
544 concentrations (8 x 10¹⁵ to 13 x 10¹⁵ molecules cm⁻²) over salt flats in Tanzania as the waters
545 of Lake Natron, a soda lake with relatively alkaline pH, recede during the dry season¹⁴⁰. A
546 similar seasonal behaviour has been observed over the Sudd wetlands in South Sudan¹⁴¹.
547 Roughly half of the Sudd wetlands are permanently flooded, with part of the remaining wetland
548 area drying each year¹⁴². The extent of drying can vary substantially from year to year. During
549 2008-2019, NH₃ concentrations over the region reached nearly 30 x 10¹⁵ molecules cm⁻² in
550 2010 when seasonal drying of the Sudd was most extensive, compared with 11 x 10¹⁵
551 molecules cm⁻² in 2014 when drying was least extensive¹⁴¹.

552

553 **4.3. Water security**

554

555 Rainfall variability has direct consequences for human wellbeing and health, including
556 generation of clean energy from hydropower, transboundary water management, urban

557 drainage, and vector-borne and water-borne diseases. A preliminary assessment by the UN
558 in 2022 of water security across Africa¹⁴³, based on a range of ten criteria including access to
559 drinking water, sanitation, and water infrastructure, highlighted that Eastern Africa includes
560 some of the lowest scoring countries.

561

562 To meet growing energy demands in Eastern Africa, hydropower development is often seen
563 as a viable solution and one that does not involve the combustion of fossil fuels. Ethiopia and
564 Sudan seek to meet domestic energy needs and aspire to market energy across the East
565 Africa Power Pool (EAPP). The current capacity of hydropower contributes about 50% of
566 electrical generation in EAPP countries, with a planned doubling of capacity over Eastern
567 Africa by 2030 that will mostly be in the Nile Basin. However, a strong dependency on
568 hydropower places the entire economic system at the mercy of variable hydrologic
569 conditions¹⁴⁴ in an increasingly uncertain climatic future^{145,146}. Linking energy networks across
570 hydrologic zones and organising infrastructure investment to be 'climate-proof' is one potential
571 solution, without which countries that rely heavily on hydropower will likely suffer from
572 fluctuating electricity prices¹⁴⁴. The EAPP helps to coordinate the trade and interconnection of
573 cross-border energy networks, but there remain significant political challenges as energy
574 needs grow with projected future increases in urbanisation, expanding irrigation plans, and
575 variable release from upstream hydropower plants^{144,147}.

576

577 While Zambia is not part of Eastern Africa it does serve as an example of the multiplicative
578 consequences of rainfall variations on hydropower, and they are part of the southern African
579 counterpart of the EAPP. Extremely dry conditions during 2015 and 2016 linked with the strong
580 El Niño led to reduced inflow into Lake Kariba that feeds into the Kariba Dam that provides
581 1,830 megawatts of hydroelectric power to Zambia and Zimbabwe. Lake levels in January
582 2016 dropped to 12% of capacity, just above the minimum necessary to generate electricity¹⁴⁸.
583 This led to major energy deficit in Zambia that was managed by buying energy from
584 neighbouring countries and by daily power outages, particularly affecting Lusaka Province and
585 the Copper Belt. This subsequently led to damage associated with a suspension of heating
586 and refrigeration and, combined with a fall in the global copper price, led to an estimated 19%
587 drop in GDP¹⁴⁹. Conversely, anomalous flooding of the Zambezi basin due to torrential rainfall
588 can overwhelm the Kariba Dam which resulted in a necessary release of water in March 2010
589 due to El Niño conditions, which affected the discharge rates of downstream dams, leading to
590 major floods that impacted hundreds of thousands of people.

591

592 More generally, variability in precipitation presents an important issue for regional water
593 security in East African countries that include transboundary rivers¹⁵⁰. There are substantial
594 challenges associated with managing critical multi-purpose infrastructures that support dams
595 for hydropower but also for agricultural expansion and flood control, especially considering
596 variations in rainfall and the associated river flows. Safely handling severe flooding and
597 drought events requires close communication between managers of different dams, some of
598 which will be across political borders, to avoid harm to co-riparian nations¹⁵¹ and to avert
599 international conflict¹⁵².

600

601 Fortunately, violent conflict between nations over shared water resources is almost non-
602 existent anywhere on the globe¹⁵³. Over Eastern Africa, minor conflicts have been mainly led
603 by herders and farmers in neighbouring countries fighting over pasture and water for livestock.

604 Construction of the Grand Ethiopian Renaissance Dam (GERD) on the Blue Nile River has
605 the potential to be the biggest risk of conflict between neighbouring Eastern African countries.
606 The dam is part of Ethiopia's economic growth plan to become Africa's largest hydropower
607 exporter. However, there is concern that GERD will reduce downstream water for irrigation
608 and drinking, and to a lesser extent reduce hydropower capacity. Years of heavy rainfall over
609 Ethiopia, such as 2020, can help fill the GERD and result in release of sufficient water to
610 Sudan and Egypt. Proponents of GERD argue that in years with lower rainfall, the dam's water
611 storage can be used to alleviate drought in downstream countries. But this relies on the dam
612 releasing the water. Diplomatic negotiations are ongoing, but the situation serves as an
613 example of the complexities associated with transboundary water.

614
615 Economic development of Eastern African countries is tied to increasing urbanization,
616 resulting in rapid expansion of cities to accommodate growing populations¹⁵⁴. This includes
617 expansion of infrastructure to support access to electricity and clean water, removal of
618 wastewater and sewage treatment, development of road networks, and improved internet and
619 cellular connectivity. Periods of intense rainfall can quickly overwhelm inadequate
620 infrastructure¹⁵⁵, resulting in overflowing drainage systems, flooded houses and suspension
621 of sewage treatment often resulting in a range of health emergencies¹⁵⁶. Flooding can also
622 damage roads and railways built with limited budgets and inadequate engineering, disrupting
623 the transportation of workers and food supplies from rural to urban areas and consequently
624 affecting economic activity¹⁵⁷.

625
626 Heavy rainfall over Sudan in 2020 led to extensive flooding that damaged or destroyed
627 112,000 homes, causing a three-month state of emergency to be declared¹⁵⁸. Heavy rains and
628 flash flooding over Sudan in 2021 affected 88,000 people in 13 out of the 18 states. Damage
629 and destruction of houses and clean water sources were widespread. Flash flooding also
630 affected the sewage systems of internally displaced persons camps in South Darfur, closed
631 schools, power plant substations, and rendered roads impassable. The frequency and
632 magnitude of heavy rainfall across Sudan will continue to prove a challenge for urban areas
633 that do not have adequate infrastructure and will ultimately compromise the economic
634 development of the region.

635
636 Rainfall is also a key component for the propagation of several vector-borne and water-borne
637 diseases relevant to Eastern Africa. The influence of temperature on the malaria parasite, for
638 example, is well understood¹⁵⁹⁻¹⁶¹ compared to the impact of intense rainfall and associated
639 flooding on the mosquito life cycle and subsequent virus transmissions. Mosquitoes and other
640 arthropods that carry malaria and arboviruses, for example, dengue, often include an aquatic
641 stage to support the development of their eggs and larvae. A number of studies have focused
642 on extreme rainfall events during the El Niño phase of ENSO during 1997/1998 and
643 2015/2016¹⁶²⁻¹⁶⁵. Other studies have linked the IOD to an increase in the risk of malaria in the
644 East African highlands^{166,167}. There are similar challenges associated with water-borne
645 diseases such as cholera and typhoid that are prevalent across Eastern Africa, and become
646 of more concern during specific shifts in rainfall and variations in temperature^{157,168,169}.
647 Combatting these viruses is exacerbated by non-climate factors, including international travel,
648 pockets of increased population density associated with urbanisation, and land-use change
649 that can move peri-urban regions closer to mosquito and arthropod breeding grounds.

650

651 Extreme rainfall associated with the strong El Niño during 1997/1998 followed an extended
652 drought period and led to an outbreak of malaria in a non-immune population of north-eastern
653 Kenya. The extent of the outbreak had not been seen since 1952. Records of hospital
654 admissions reported a three-month lag after heavy rainfall in November 1997 (ref ¹⁶²). Hospital
655 data from one community reported a ten-fold increase in expected daily rates of crude and
656 under-five mortality¹⁶², which rapidly reduced by the end of April 1998 when rainfall subsided.
657 A similar story was reported for a district in western Uganda¹⁶³. For communities of the
658 Tanzanian highlands, however, researchers found a marked reduction in malaria cases in
659 1997/1998 compared to previous years. This reduction was attributed to flooding which can
660 flush mosquito larvae from breeding sites thereby decreasing the disease spread¹⁷⁰. Two out
661 of the three communities that reported an increase in malaria after the heavy rains were
662 located next to a body of standing water that is an ideal breeding ground for mosquitoes¹⁷⁰.
663 More generally, periods of heavy rainfall whether they are associated with El Niño or the IOD,
664 result in human health challenges for local communities that are overwhelmed by floods that
665 lead to pools of standing water^{164,165}.

666

667 We have described a few of the many impacts associated with rainfall extremes over Eastern
668 Africa. Trends and variations in rainfall are linked with, and therefore difficult to separate from,
669 changes in temperature. Concurrent changes in temperature^{171–173} can reinforce or weaken¹⁷⁴
670 impacts due to rainfall.

671

672 **5 Future changes**

673

674 Given the multifarious impacts of rainfall changes over Eastern Africa, there is a need to
675 consider how rainfall and its drivers might change in the future. This knowledge provides
676 actionable information with which to develop effective mitigation strategies.

677

678 *Rainfall*

679

680 Projected future changes in Eastern African climate have been studied using global (GCM)
681 and regional (RCM) Earth System models (ESMs)^{18,48,175–181}, each with considerable spread
682 amongst ensemble members and models, casting doubt on the reliability of projections⁵⁷.
683 Unfortunately, there are also limited relationships between the abilities of individual models to
684 describe past and future east African climate and the model spread¹⁸². Hence, constraining
685 future projections simply by observation of current day ESM performance is not possible.

686

687 These model limitations are particularly evident for the long rains when GCMs and RCMs
688 show substantial inter- and intra-model differences, resulting in a diversity of projected
689 responses and thus uncertainty. Indeed, GCMs report no significant change¹⁷⁹, a decrease¹⁸³
690 and a small increase in the long rains under anthropogenic warming, consistent with the range
691 of responses for CMIP5 models^{176,184}. CMIP6 model calculations also exhibit variability, with
692 the multi-model ensemble providing hints of a small increase in the long rains for Eastern
693 Africa (the sum of IPCC southeast and northeast Africa regions) (**Fig. 4a**). Under SSP2-4.5,
694 for example, the multi-model median projects statistically significant 0.02 mm day⁻¹ decade⁻¹
695 increases (2015-2100), although changes only really emerge after ~2080. These increases
696 are also sensitive to the emission scenario used, as demonstrated by a larger positive trend
697 (0.06 mm day⁻¹ decade⁻¹, 2015-2100) under SSP5-8.5 (**Fig. 4b**), which also tend to emerge
698 earlier (~2040). In contrast, CORDEX¹⁸⁵ regional models support no such increase in the long

699 rains, instead exhibiting a statistically significant slight negative trend for RCP4.5 (-0.01mm
700 day⁻¹ decade⁻¹, 2006-2100; **Fig. 4c**), and a statistically insignificant slight positive trend for
701 RCP8.5 (**Fig. 4d**). Based on these calculations, there is no clear indication regarding the sign
702 and magnitude of future long rain changes over east Africa, nor their potential drivers. These
703 minimal changes in long rains have been attributed to the continental thermal, centred near
704 the equator and present during the long rains, being insensitive to changes in subtropical
705 atmospheric hydrodynamics driven by rising atmospheric GHG during the 21st century¹³.

706
707 These models generally exhibit better inter- and intra- model agreement for the short rains¹⁷⁶,
708 albeit still with substantial spread, providing some confidence in the projected future climate
709 states. Indeed, the short rains are projected to increase with anthropogenic warming^{18,179,183}.
710 Under SSP2-4.5, the CMIP6 ensemble projects a statistically significant 0.04mm day⁻¹ decade⁻¹
711 (2015-2100) increase in the short rains, the increase emerging in ~2040 (**Fig. 4a**). These
712 changes are more pronounced under SSP5-8.5 for the same period, wherein trends of 0.11
713 mm day⁻¹ decade⁻¹ are projected, emerging earlier¹⁸ (~2030-2040) (**Fig. 4b**). CORDEX
714 simulations exhibit a similar pattern: a small but statistically significant increase for RCP4.5
715 (0.03 mm day⁻¹ decade⁻¹, 2006-2100; **Fig. 4c**), and a stronger response that emerges earlier
716 for RCP8.5 for the same period (0.05mm day⁻¹ decade⁻¹; **Fig. 4d**). A convection-permitting
717 regional model also supports these findings, additionally reporting a large increase in extreme
718 rainfall rates during the short rains¹⁸⁶. The magnitude and large spatial extent of this increase
719 in extreme rainfall were underestimated by the corresponding regional models using
720 parametrised convection (including CMIP5, CMIP6 and CORDEX simulations) so they may
721 be underpredicting the full extent of future increases in rainfall intensity across Eastern
722 Africa¹⁸⁶.

723
724 This increase in the short rains arises from increased moisture convergence over Eastern
725 Africa¹⁷⁹. This enhanced moisture convergence emerges from increased atmospheric
726 moisture¹⁷⁹ due to a warming climate and from anomalous circulation patterns associated with
727 a strengthening in the continental low over southern Africa and the subtropical high over the
728 South Indian Ocean, and a weakening of the eastern Sahara subtropical high. A weakening
729 of the Walker circulation in response to warming SSTs over the western Indian Ocean also
730 favours an upward trend in the short rains^{48,183}. Nevertheless, limitations in model
731 representations of key processes and climatologies—for example, overestimates in the short
732 rains and underestimates in the long rains¹⁸⁷, an unrealistic dominance of the Walker
733 circulation¹⁸⁸, and failure to reproduce the observed SST gradient across the equatorial
734 Pacific⁵⁷—all cast doubt on rainfall projections and understanding of their corresponding
735 drivers. With these caveats in mind, conclusions are limited to saying that the rainfall during
736 the short rains is increasing at a faster rate than the long rains (**Fig. 4**).

737 738 *ENSO and IOD*

739
740 ENSO and the IOD have had a dominant influence on rainfall variations across Eastern Africa.
741 It is therefore instructive to understand their future projections in the hope of informing rainfall
742 projections. As with rainfall itself, there is often a lack of consensus regarding how these
743 modes of variability will change under anthropogenic warming. For ENSO¹⁸⁹, no significant
744 change in intensity and frequency has been reported in some instances^{190–192}, while an
745 increased occurrence of extreme El Niño and La Niña events is reported by others^{193–195}.
746 Similarly, no significant change in the overall frequency and amplitude of the IOD is projected

747 by coupled models^{196,197}, although the frequency of extreme positive IOD events is thought to
748 increase^{193,198}. Assuming present-day relationships between Eastern African rainfall and
749 ENSO and IOD remain the same in the future, the short rains would then become wetter with
750 an increasing chance of torrential rains and associated higher risk of flooding.

751

752 However, even if the frequency and intensity of ENSO and IOD do not change in a warming
753 climate, there is some consensus about how these climatic modes of variability will remotely
754 influence the future climate system. For instance, rainfall extremes associated with ENSO and
755 IOD can be expected to be more severe in a warming world owing to an intensified hydrologic
756 cycle¹⁹⁹. Moreover, faster warming is expected in the western and eastern Indian Ocean
757 compared to surrounding bodies of water^{193,196,200}. Because of these shifts, the tropical oceans
758 will tend towards an El Niño-like and positive IOD-like state, associated with weakening of the
759 Walker circulation, shifts in the ITCZ²⁰¹ and an increase in atmospheric moist static energy.
760 Consequently, as a result of changing background SSTs and circulation shifts during the short
761 rains later this century, ENSO and IOD are expected to have a stronger coupling with rainfall
762 over the Horn of Africa but a weaker coupling with rainfall over the southern part of Eastern
763 Africa¹⁸³. The long rains, which are historically insensitive to remote SST forcing, would then
764 become substantially more responsive to ENSO in future projections¹⁸³. Model projections
765 also suggest an enhanced La Niña-related rainfall anomaly over Eastern Africa during July-
766 September compared to the present period¹⁸³.

767

768 Uncertainty about future changes in ENSO and IOD, combined with potential changes in the
769 strength of teleconnections results in considerable uncertainty around changes in future
770 rainfall over Eastern Africa driven by ENSO and the IOD. If the frequency of extreme positive
771 IOD events increases^{193,198}, and the strength of the teleconnection increases over Eastern
772 Africa¹⁸³, this may result in wetter conditions over eastern Eastern Africa during the short rains.
773 Changes in the frequency of El Niño and La Niña events, coupled with increasing sensitivity
774 to ENSO during the long rains and summer rainfall seasons may lead to increasing variability
775 in these seasons in the future. Additionally, increases in the frequency of extreme El Niño and
776 La Niña events, and increasing teleconnection strength, may increase the frequency of
777 extreme rainfall seasons throughout the year.

778

779 *Impacts*

780 As in the present climate, any future changes in seasonal rainfall across Eastern Africa will
781 result in a wide range of economic and humanitarian impacts.

782

783 Changes in agricultural yields due to changing rainfall patterns are crop dependent. Current
784 understanding of future crop yields is more sensitive to uncertainties in temperature than
785 rainfall¹⁷² due to crops generally having an optimal growing temperature range, outside of
786 which the yield falls off rapidly^{173,202}. Optimal yields also rely on adequate soil moisture that
787 helps to regulate available water in the plant root zone²⁰³. Changes in the timing, duration, and
788 magnitude of the long and short rains (Figure 4) will also need to be considered by farmers
789 when they decide which crops and seed-types are grown throughout the year²⁰⁴. Increased
790 frequency of extreme rainfall events will result in flooding that leads to damaged crops¹⁴ and
791 agricultural infrastructure that raises concerns about food security. Availability of water and
792 food will also influence livestock production²⁰⁵.

793

794 Anthropogenic warming will also induce changes to large-scale biogeochemical cycles across
795 Eastern Africa, with the possibility to feedback on atmospheric GHG concentrations¹²³. Indeed,
796 the impact of precipitation variability on contemporary wetland methane emissions, is
797 expected to continue in the future. For instance, CMIP5 simulations (Supplementary
798 Information) predict methane emissions will increase by ~4Tg yr⁻¹ under RCP4.5 and ~11 Tg
799 yr⁻¹ for RCP8.5 from 2000 to 2100 (**Fig. 5a, b**). These projected increases can be linked to
800 increases in surface temperature, inundation (via rainfall) and net primary production
801 (including indirect effects through rainfall), each with similar importance (**Fig. 5c**). Moreover,
802 future rainfall variability, namely the projected increase in short rains, is expected to reduce
803 the spatial extent of fires²⁰⁶ and enhance above-ground biomass (and associated vegetation
804 greening²⁰⁷ and increase in NPP²⁰⁸) with an accompanying transition to forest biomes over
805 East Africa^{209–211}. These changes will each have subsequent effects on ecosystem
806 functioning, carbon cycling and broader biogeochemical narratives in the Earth System.

807

808 There is a threshold of relative humidity (and temperature) that limits the transmission of
809 malaria and arboviruses via their influence on the associated vectors (for example,
810 mosquitoes) and pathogens^{168,212,213}. Increases in relative humidity associated with more
811 extreme wet seasons in the future can shorten the incubation and blood-feeding stages²¹³ of
812 the mosquito life cycle, but the net impact of these changes is unclear. Increased future levels
813 of rainfall and its variability may also lead to more frequent and persistent flooding that will
814 help establish more breeding sites for insects, although some vectors breed indoors and will
815 be unaffected directly by flooding. The relationship between flooding and water-borne
816 diseases such as cholera and typhoid differs by region^{168,212}. However, one of the biggest risks
817 for future transmission of malaria and arboviruses in Eastern Africa is drug and insecticide
818 resistance combined with warmer temperatures and lower relative humidity associated with
819 climate change in the highland regions, where there is little immunity and insufficient health
820 infrastructure^{160,161,214,215}.

821

822 **6 Summary & future perspectives**

823

824 Eastern Africa suffers extreme seasonal and year-to-year variations in rainfall, driving
825 substantial environmental, social, and economic impacts. For instance, extreme changes in
826 hydroclimatic conditions during 2021, exacerbated by water management challenges, have
827 led to some of the worst flooding in South Sudan for the past sixty years, impacting food and
828 energy security, access to potable water, and the spread of waterborne disease and
829 arboviruses. Other parts of Eastern Africa, particularly countries in the Horn of Africa, are
830 experiencing prolonged and extensive drought due to consecutive La Niña events from 2020-
831 2022, exacerbated by GHG warming over the western Pacific. These droughts have resulted
832 in the collapse of agricultural crops and livestock that support subsistence farming across the
833 region.

834

835 While uncertain, there is some consensus that short rains totals (OND) will exceed those of
836 the long rains (MAM) in a warming climate, the timing of which is dependent on the scenario
837 but could occur as early as 2030. Regional climate models generally show a stronger rainfall
838 response to a warming climate, with models that resolve convection reporting even higher
839 extreme rainfall rates. This suggests that the vast majority of climate model, which still use
840 parametrised convection, are potentially underpredicting future increases in rainfall and
841 therefore the subsequent impacts across Eastern Africa.

842
843
844
845
846
847
848
849
850
851
852
853
854
855
856
857
858
859
860
861
862
863
864
865
866
867
868
869
870
871
872
873
874
875
876
877
878
879
880
881
882
883
884
885
886
887
888
889

To minimize the risks associated with extreme variations in rainfall over Eastern Africa, several priority areas of future research are required, all demanding the development of proactive policies.

Improve meteorological observing networks and forecast systems

Improved early detection and weather forecast systems that focus on Eastern Africa will engender better preparedness for extremes associated with seasonal changes in rainfall and will inform decadal planning strategies. Development and evaluation of convective-permitting regional climate models¹⁸⁶ would provide further confidence in their ability to describe extreme rainfall events that have disproportionately important impacts. Growing model skill in sub-seasonal rainfall forecasts^{216–222} relies on improving model physics of the atmosphere and ocean, and on more and higher-quality data, particular from satellites that include instruments that observe atmosphere and ocean properties. Improved model simulations of the long rains over Eastern Africa hinge on improving knowledge of the atmospheric state, particularly the humidity over the Northwest Indian Ocean²²³, which could be tested with a dedicated measurement campaign. Ocean interior measurements currently collected by arrays of buoys across the tropics, particularly the Indian Ocean and western Pacific, could be expanded to help reduce knowledge gaps²²⁴. To improve forecast skill of high-impact weather events over Eastern Africa, targeted²²⁵ ground-based, airborne and shipborne observations could be deployed to supplement existing operational data streams. Equally important are the assimilation methods that optimise the use of these observations for improving model simulations²²⁶.

Translating forecast analyses into actionable information is a key part of any system^{227,228}. The Famine Early Warning Systems Network⁸¹ is a good example of such a system. Delivering useful information to countries requires detailed knowledge about national agricultural and economic policies, evolving national political environments and the capability to communicate with local farming communities and governments. Establishing long-term funding that supports civilian data collecting, transcending lifecycles of individual governments, will help to provide effective information about how to mitigate the worst climate impacts.

Improve environmental observing systems

Climate and weather forecast data can also help with disease forecasting¹⁵⁹ but this has not yet been fully realised. Satellite observations of surface temperature, humidity and land use change can be used to predict shifts in disease burden²²⁹ and hotspots for emerging zoonotic diseases and how they will spread^{230–232}, and together with epidemiological data could form the basis of early detection systems over Eastern Africa¹⁵⁹.

Understanding quantitative changes in hydrology and the carbon cycle across Eastern Africa is currently limited to very few surface sites and broad inferences from satellite observations^{120,233}. Given the importance of water flows across the regions and subsequent impacts on water and food security and the carbon cycle there is a clear need for a more coordinated and sustainable measurement network to monitor variations²³⁴. More collaboration between African and international hydrologists, ecologists, and carbon cycle scientists will help facilitate this kind of activity.

890 Advanced Earth System Models

891 Exploiting advances in observing systems and better understanding the carbon-water nexus
892 must translate into commensurate improvements²²⁷ in physically based simulations of East
893 African climate, and how it relates to the broader climate system. A key recommendation is to
894 develop a more robust understanding of the relationship between future levels of atmospheric
895 GHG and changes in the frequency and variability of the IOD^{67,193,196,198,235,236}, and how future
896 changes in ENSO and the IOD will influence rainfall over Eastern Africa¹⁸³ and in turn how
897 that influences vegetation cover and subsequently the emission of methane¹²³. This point ties
898 together the previous recommendations, and only by bringing together communities involved
899 in measurements and model development can meaningful progress be made with identifying
900 and prioritizing work on sources of uncertainty.

901

902 Improve freshwater security

903 Eastern Africa encompasses countries that are being flooded and countries that are subject
904 to drought, both driven by large inter- and intra-seasonal changes in rainfall. In both extremes,
905 there is an urgent need to improve national water storage and sanitation plants to improve the
906 safety and security of freshwater resources to support increased agricultural output and a
907 growing population²³⁷. This is a systemic challenge that requires co-development of water
908 usage strategies between stakeholders and experts, informed by scenarios that account for
909 changes in rainfall, land use, and the growing demands from an increase in population.
910 Recommendations include investment in water-saving technologies and management options
911 such as the adoption of sprinkler and drip irrigation systems to replace commonly-used flood
912 irrigation, and to invest in recycling wastewater when surface or groundwater reserves are
913 insufficient²³⁷. Such an approach should also consider upstream and downstream water
914 demands and losses, including the reduction of evaporative loss from catchment lakes²³⁸ and
915 the potential downsides of adopting different approaches²³⁹.

916

917 Ensure food security

918 Ensuring future food security is related to the security of freshwater, with the agriculture sector
919 generally having the lowest water use efficiency of all the water-using sectors²⁴⁰.

920

921 How this sector will cope with changes in rainfall variability will depend on the nature of those
922 changes. An upward trend in rainfall in some countries for different seasons, with an
923 accompanying warming trend, may benefit some food crops that have a higher optimal
924 growing temperature. However, if increased rainfall results from a higher frequency of extreme
925 rainfall events that follow periods of drought, then flooding will become more of a challenge.
926 Investment in better drainage systems is one solution, but in the longer term an increase in
927 flooded areas that can be managed may provide an opportunity to increase the use of
928 floodplain agriculture, spate irrigation²⁴¹ or inundation canals. A shift in rainfall and surface
929 water catchment areas may result in a redistribution of crops being grown across Eastern
930 Africa. Countries that will suffer from more extensive droughts have other challenges to face.
931 In this case, the agricultural sector should invest in more efficient water management systems,
932 as described above, and distributing drought-tolerant seeds²⁴² to maximize agricultural crop
933 yields during drought years. Widespread adoption of conservation tillage methods would
934 reduce water and soil loss, mainly by decreasing the intensity of the tillage and retention of
935 post-harvest plant residue²⁴³. Development of agricultural strategies to help farmers maximize
936 food production during good years would help mitigate impacts during drought years. Institutes

937 affiliated with the Consultative Group on International Agricultural Research continue to play
938 a key role in addressing those sustainable agricultural challenges.

939
940 All these recommendations require unprecedented levels of coordination and substantial
941 financial investment to link local to national scales, and in many cases will require trans-
942 boundary cooperation that will also involve extensive international diplomacy. Some activities
943 are underway, but some countries may require international financial aid to establish larger
944 activities that will eventually become self-sustaining. Without properly addressing the bigger
945 challenges now it becomes progressively more difficult for Eastern African countries to cope
946 with future variations in rainfall without incurring substantial humanitarian and economic
947 costs²⁴⁴ that will dwarf the multi-trillion dollar cost of the Covid-19 pandemic.

948 **Acknowledgements**

949 P.I.P., L.F. and M.L. acknowledge support from the UK National Centre for Earth Observation
950 (NCEO) funded by the National Environment Research Council (NE/R016518/1). C.W.
951 acknowledges funding of the Grantham Research Fellowship from the Grantham Foundation.
952 K.W. acknowledges Oxford Martin Programme on Transboundary Resource Management. B.
953 Dong and K. Haines acknowledge support of the NCEO LTS-S and International Programme
954 (NE/X006328/1).
955

956 **Author contributions**

957 P.I.P. originated the review and coordinated the writing. P.I.P., C.M.W., B.D., R.I.M., K.G.W.,
958 N.G., J.E.H., N.M. and S.S.F. led the writing of individual subsections, with contributions from
959 R.P.A., C.M.W., B.D., R.I.M., N.G. and S.S.F. provided the figures. All authors helped to revise
960 and refine earlier drafts.
961

962 **Competing interests**

963 The authors declare no competing interests.
964

965 **References**

- 966
967
- 968 1. Gamoyo, M., Reason, C. & Obura, D. Rainfall variability over the East African coast.
969 *Theor. Appl. Climatol.* **120**, (2015).
 - 970 2. Conway, D., Dalin, C., Landman, W. A. & Osborn, T. J. Hydropower plans in eastern
971 and southern Africa increase risk of concurrent climate-related electricity supply
972 disruption. *Nat. Energy* **2**, 946–953 (2017).
 - 973 3. Ferrer, N. *et al.* Groundwater hydrodynamics of an Eastern Africa coastal aquifer,
974 including La Niña 2016–17 drought. *Sci. Total Environ.* **661**, (2019).
 - 975 4. Taylor, R. G. *et al.* Evidence of the dependence of groundwater resources on extreme
976 rainfall in East Africa. *Nat. Clim. Chang.* **3**, (2013).
 - 977 5. Food Security and Nutrition Analysis Unit and Famine Early Warning System
978 Network. Somalia FSNAU Food Security & Nutrition Quarterly Brief - Focus on Post
979 Gu 2017 Season Early Warning. (2022).
 - 980 6. World Bank Group. *Somalia drought impact and needs assessment : synthesis report.*
981 (2018).
 - 982 7. Food Security and Nutrition Analysis Unit. Somalia faces Risk of Famine (IPC Phase
983 5) as multi-season drought and soaring food prices lead to worsening acute food
984 insecurity and malnutrition. <https://fsnau.org/node/1947> (2022).
 - 985 8. UN OCHA. *Humanitarian Needs Overview South Sudan. Humanitarian Programme*
986 *Cycle 2021* (2021).

- 987 9. Thomas, E. A. *et al.* Quantifying increased groundwater demand from prolonged
988 drought in the East African Rift Valley. *Sci. Total Environ.* **666**, (2019).
- 989 10. Elagib, N. A. *et al.* Debilitating floods in the Sahel are becoming frequent. *J. Hydrol.*
990 **599**, 126362 (2021).
- 991 11. Adhikari, U., Nejadhashemi, A. P. & Woznicki, S. A. Climate change and eastern
992 Africa: a review of impact on major crops. *Food Energy Secur.* **4**, 110–132 (2015).
- 993 12. Megersa, B. *et al.* Livestock Diversification: An Adaptive Strategy to Climate and
994 Rangeland Ecosystem Changes in Southern Ethiopia. *Hum. Ecol.* **42**, (2014).
- 995 13. Cook, K. H., Fitzpatrick, R. G. J., Liu, W. & Vizzy, E. K. Seasonal asymmetry of
996 equatorial East African rainfall projections: understanding differences between the
997 response of the long rains and the short rains to increased greenhouse gases. *Clim.*
998 *Dyn.* **55**, (2020).
- 999 14. Wainwright, C. M., Finney, D. L., Kilavi, M., Black, E. & Marsham, J. H. Extreme
1000 Rainfall in East Africa October 2019 - January 2020 and context under Future Climate
1001 Change. *Weather (under Rev.)* (2020).
- 1002 15. Black, E., Slingo, J. & Sperber, K. R. An observational study of the relationship
1003 between excessively strong short rains in coastal East Africa and Indian ocean SST.
1004 *Mon. Weather Rev.* **131**, (2003).
- 1005 16. MacLeod, D., Graham, R., O'Reilly, C., Otieno, G. & Todd, M. Causal pathways
1006 linking different flavours of ENSO with the Greater Horn of Africa short rains. *Atmos.*
1007 *Sci. Lett.* **22**, (2021).
- 1008 17. Indeje, M., Semazzi, F. H. M. & Ogallo, L. J. ENSO signals in East African rainfall
1009 seasons. *Int. J. Climatol.* **20**, (2000).
- 1010 18. Wainwright, C. M., Marsham, J. H., Rowell, D. P., Finney, D. L. & Black, E. Future
1011 changes in seasonality in east africa from regional simulations with explicit and
1012 parameterized convection. *J. Clim.* **34**, (2021).
- 1013 19. Nicholson, S. E. Long-term variability of the East African 'short rains' and its links to
1014 large-scale factors. *Int. J. Climatol.* **35**, (2015).
- 1015 20. Jiang, Y., Zhou, L., Roundy, P. E., Hua, W. & Raghavendra, A. Increasing Influence of
1016 Indian Ocean Dipole on Precipitation Over Central Equatorial Africa. *Geophys. Res.*
1017 *Lett.* **48**, (2021).
- 1018 21. Funk, C. *et al.* Examining the role of unusually warm Indo-Pacific sea-surface
1019 temperatures in recent African droughts. *Q. J. R. Meteorol. Soc.* **144**, (2018).
- 1020 22. Shaaban, A. A. & Roundy, P. E. OLR perspective on the Indian Ocean Dipole with
1021 application to East African precipitation. *Q. J. R. Meteorol. Soc.* **143**, (2017).
- 1022 23. Zaitchik, B. F. Madden-Julian Oscillation impacts on tropical African precipitation.
1023 *Atmospheric Research* vol. 184 (2017).
- 1024 24. Pohl, B. & Camberlin, P. Influence of the Madden-Julian Oscillation on East African
1025 rainfall. II. March-May season extremes and interannual variability. *Q. J. R. Meteorol.*
1026 *Soc.* **132**, (2006).
- 1027 25. Pohl, B. & Camberlin, P. Influence of the Madden-Julian Oscillation on East African
1028 rainfall. I: Intraseasonal variability and regional dependency. *Q. J. R. Meteorol. Soc.*
1029 **132**, (2006).
- 1030 26. Finney, D. L. *et al.* The effect of westerlies on East African rainfall and the associated
1031 role of tropical cyclones and the Madden–Julian Oscillation. *Q. J. R. Meteorol. Soc.*
1032 **146**, (2020).
- 1033 27. Berhane, F. & Zaitchik, B. Modulation of daily precipitation over East Africa by the
1034 Madden-Julian oscillation. *J. Clim.* **27**, (2014).
- 1035 28. Vellinga, M. & Milton, S. F. Drivers of interannual variability of the East African “Long
1036 Rains”. *Q. J. R. Meteorol. Soc.* **144**, (2018).
- 1037 29. Martin, Z. *et al.* The influence of the quasi-biennial oscillation on the Madden–Julian
1038 oscillation. *Nature Reviews Earth and Environment* vol. 2 (2021).
- 1039 30. Gelaro, R. *et al.* The modern-era retrospective analysis for research and applications,
1040 version 2 (MERRA-2). *J. Clim.* **30**, 5419–5454 (2017).
- 1041 31. Huesmann, A. S. & Hitchman, M. H. The stratospheric quasi-biennial oscillation in the

- 1042 NCEP reanalyses: Climatological structures. *J. Geophys. Res. Atmos.* **106**, (2001).
1043 32. Indeje, M. & Semazzi, F. H. M. Relationships between QBO in the lower equatorial
1044 stratospheric zonal winds and East African seasonal rainfall. *Meteorol. Atmos. Phys.*
1045 **73**, (2000).
1046 33. Liu, W., Cook, K. H. & Vizy, E. K. Influence of Indian Ocean SST regionality on the
1047 East African short rains. *Clim. Dyn.* **54**, (2020).
1048 34. Dyer, E. & Washington, R. Kenyan long rains: A subseasonal approach to process-
1049 based diagnostics. *J. Clim.* **34**, (2021).
1050 35. Kilavi, M. *et al.* Extreme Rainfall and Flooding over Central Kenya Including Nairobi
1051 City during the Long-Rains Season 2018: Causes, Predictability, and Potential for
1052 Early Warning and Actions. *Atmosphere (Basel)*. **9**, 472 (2018).
1053 36. Kebacho, L. L. The Role of Tropical Cyclones Idai and Kenneth in Modulating Rainfall
1054 Performance of 2019 Long Rains over East Africa. *Pure Appl. Geophys.* (2022)
1055 doi:10.1007/s00024-022-02993-2.
1056 37. Kebacho, L. L. Interannual variations of the monthly rainfall anomalies over Tanzania
1057 from March to May and their associated atmospheric circulations anomalies. *Nat.*
1058 *Hazards* (2022).
1059 38. Tarnavsky, E. *et al.* Extension of the TAMSAT satellite-based rainfall monitoring over
1060 Africa and from 1983 to present. *J. Appl. Meteorol. Climatol.* **53**, (2014).
1061 39. Maidment, R. I. *et al.* A new, long-term daily satellite-based rainfall dataset for
1062 operational monitoring in Africa. *Sci. Data* **4**, (2017).
1063 40. Dai, A. Hydroclimatic trends during 1950–2018 over global land. *Clim. Dyn.* **56**,
1064 (2021).
1065 41. Maidment, R. I., Allan, R. P. & Black, E. Recent observed and simulated changes in
1066 precipitation over Africa. *Geophys. Res. Lett.* **42**, (2015).
1067 42. Cattani, E., Merino, A., Guijarro, J. A. & Levizzani, V. East Africa Rainfall trends and
1068 variability 1983-2015 using three long-term satellite products. *Remote Sens.* **10**,
1069 (2018).
1070 43. Maidment, R. I. *et al.* The 30 year TAMSAT african rainfall climatology and time series
1071 (TARCAT) data set. *J. Geophys. Res.* **119**, (2014).
1072 44. Liebmann, B. *et al.* Climatology and interannual variability of boreal spring wet season
1073 precipitation in the eastern horn of Africa and implications for its recent decline. *J.*
1074 *Clim.* **30**, 3867–3886 (2017).
1075 45. Wainwright, C. M. *et al.* Eastern African Paradox rainfall decline due to shorter not
1076 less intense Long Rains. *npj Clim. Atmos. Sci.* **2**, (2019).
1077 46. Walker, D. P., Marsham, J. H., Birch, C. E., Scaife, A. A. & Finney, D. L. Common
1078 Mechanism for Interannual and Decadal Variability in the East African Long Rains.
1079 *Geophys. Res. Lett.* **47**, (2020).
1080 47. Nicholson, S. E. Climate and climatic variability of rainfall over eastern Africa. *Rev.*
1081 *Geophys.* **55**, (2017).
1082 48. Tierney, J. E., Ummenhofer, C. C. & deMenocal, P. B. Past and future rainfall in the
1083 Horn of Africa. *Sci. Adv.* **1**, e1500682 (2015).
1084 49. Saji, N. H., Goswami, B. N., Vinayachandran, P. N. & Yamagata, T. A dipole mode in
1085 the tropical Indian Ocean. *Nature* **401**, 360–363 (1999).
1086 50. Webster, P. J., Moore, A. M., Loschnigg, J. P. & Leben, R. R. Coupled ocean-
1087 atmosphere dynamics in the Indian Ocean during 1997-98. *Nature* **401**, (1999).
1088 51. Funk, C. *et al.* Examining the potential contributions of extreme ‘western v’ sea
1089 surface temperatures to the 2017 March-June east african drought. *Bull. Am.*
1090 *Meteorol. Soc.* **100**, (2019).
1091 52. Liebmann, B. *et al.* Climatology and interannual variability of boreal spring wet season
1092 precipitation in the eastern horn of Africa and implications for its recent decline. *J.*
1093 *Clim.* **30**, (2017).
1094 53. Thielke, A. & Mölg, T. Observed and simulated Indian Ocean Dipole activity since the
1095 mid-19th century and its relation to East African short rains. *Int. J. Climatol.* **39**,
1096 (2019).

- 1097 54. Trenberth, K. E., Fasullo, J. T., Branstator, G. & Phillips, A. S. Seasonal aspects of
1098 the recent pause in surface warming. *Nat. Clim. Chang.* **4**, (2014).
- 1099 55. L’Heureux, M. L., Lee, S. & Lyon, B. Recent multidecadal strengthening of the Walker
1100 circulation across the tropical Pacific. *Nat. Clim. Chang.* **3**, (2013).
- 1101 56. England, M. H. *et al.* Recent intensification of wind-driven circulation in the Pacific and
1102 the ongoing warming hiatus. *Nat. Clim. Chang.* **4**, (2014).
- 1103 57. Seager, R. *et al.* Strengthening tropical Pacific zonal sea surface temperature
1104 gradient consistent with rising greenhouse gases. *Nature Climate Change* vol. 9
1105 (2019).
- 1106 58. Black, E. The relationship between Indian Ocean sea-surface temperature and East
1107 African rainfall. *Philos. Trans. R. Soc. A Math. Phys. Eng. Sci.* **363**, (2005).
- 1108 59. Lyon, B. Seasonal drought in the Greater Horn of Africa and its recent increase during
1109 the March-May long rains. *J. Clim.* **27**, (2014).
- 1110 60. Allan, R. P. *et al.* Advances in understanding large-scale responses of the water cycle
1111 to climate change. *Annals of the New York Academy of Sciences* vol. 1472 (2020).
- 1112 61. Bronnimann, S. *et al.* Southward shift of the northern tropical belt from 1945 to 1980.
1113 *Nat. Geosci.* **8**, (2015).
- 1114 62. Undorf, S. *et al.* Detectable Impact of Local and Remote Anthropogenic Aerosols on
1115 the 20th Century Changes of West African and South Asian Monsoon Precipitation. *J.*
1116 *Geophys. Res. Atmos.* **123**, (2018).
- 1117 63. Dong, B. & Sutton, R. Dominant role of greenhouse-gas forcing in the recovery of
1118 Sahel rainfall. *Nat. Clim. Chang.* **5**, (2015).
- 1119 64. Blau, M. T. & Ha, K. J. The Indian Ocean Dipole and its Impact on East African Short
1120 Rains in Two CMIP5 Historical Scenarios With and Without Anthropogenic Influence.
1121 *J. Geophys. Res. Atmos.* **125**, (2020).
- 1122 65. Kew, S. F. *et al.* Impact of precipitation and increasing temperatures on drought
1123 trends in eastern Africa. *Earth Syst. Dyn.* **12**, (2021).
- 1124 66. Held, I. M. & Soden, B. J. Robust responses of the hydrological cycle to global
1125 warming. *J. Clim.* **19**, (2006).
- 1126 67. Vecchi, G. A. & Soden, B. J. Global warming and the weakening of the tropical
1127 circulation. *J. Clim.* **20**, (2007).
- 1128 68. Byrne, M. P. & Schneider, T. Narrowing of the ITCZ in a warming climate: Physical
1129 mechanisms. *Geophys. Res. Lett.* **43**, (2016).
- 1130 69. Byrne, M. P., Pendergrass, A. G., Rapp, A. D. & Wodzicki, K. R. Response of the
1131 Intertropical Convergence Zone to Climate Change: Location, Width, and Strength.
1132 *Current Climate Change Reports* vol. 4 (2018).
- 1133 70. Ayana, E. K., Ceccato, P., Fisher, J. R. B. & DeFries, R. Examining the relationship
1134 between environmental factors and conflict in pastoralist areas of East Africa. *Sci.*
1135 *Total Environ.* **557–558**, (2016).
- 1136 71. Nakawuka, P., Langan, S., Schmitter, P. & Barron, J. A review of trends, constraints
1137 and opportunities of smallholder irrigation in East Africa. *Glob. Food Sec.* **17**, 196–212
1138 (2018).
- 1139 72. Alter, R. E., Im, E. S. & Eltahir, E. A. B. Rainfall consistently enhanced around the
1140 Gezira Scheme in East Africa due to irrigation. *Nat. Geosci.* **8**, (2015).
- 1141 73. Vicente-Serrano, S. M. *et al.* Challenges for drought mitigation in Africa: The potential
1142 use of geospatial data and drought information systems. *Appl. Geogr.* **34**, (2012).
- 1143 74. Mera, G. A. Drought and its impacts in Ethiopia. *Weather Clim. Extrem.* **22**, 24–35
1144 (2018).
- 1145 75. Funk, C. Ethiopia, Somalia and Kenya face devastating drought. *Nature* **586**, 645
1146 (2020).
- 1147 76. Korecha, D. & Barnston, A. G. Predictability of June-September rainfall in Ethiopia.
1148 *Mon. Weather Rev.* **135**, (2007).
- 1149 77. Bachewe, F. N., Yimer, F., Minten, B. & Dorosh, P. A. *Agricultural prices during*
1150 *drought in Ethiopia. ESSP Working Paper* vol. 97 (2016).
- 1151 78. Obasi, G. O. P. The impacts of ENSO in Africa. in *Climate Change and Africa* vol.

- 1152 9780521836340 (2005).
- 1153 79. Desta, Z. H. & Oba, G. Feed scarcity and livestock mortality in enset farming systems
1154 in the Bale highlands of southern Ethiopia. *Outlook Agric.* **33**, (2004).
- 1155 80. Habte, M., Eshetu, M., Maryo, M., Andualem, D. & Legesse, A. Effects of climate
1156 variability on livestock productivity and pastoralists perception: The case of drought
1157 resilience in Southeastern Ethiopia. *Vet. Anim. Sci.* **16**, (2022).
- 1158 81. Funk, C. *et al.* Recognizing the famine early warning systems network over 30 years
1159 of drought early warning science advances and partnerships promoting global food
1160 security. *Bull. Am. Meteorol. Soc.* **100**, (2019).
- 1161 82. Novella, N. S. & Thiaw, W. M. African rainfall climatology version 2 for famine early
1162 warning systems. *J. Appl. Meteorol. Climatol.* **52**, 588–606 (2013).
- 1163 83. Backer, D. & Billing, T. Validating Famine Early Warning Systems Network projections
1164 of food security in Africa, 2009–2020. *Glob. Food Sec.* **29**, (2021).
- 1165 84. Simtowe, F. *et al.* Heterogeneous seed access and information exposure: implications
1166 for the adoption of drought-tolerant maize varieties in Uganda. *Agric. Food Econ.* **7**,
1167 (2019).
- 1168 85. Philip, S. *et al.* The drought in Ethiopia, 2015. *Clim. Dev. Knowl. Netw. World Weather*
1169 *Attrib. Initiat.* (2017).
- 1170 86. Toreti, A. *et al.* *Drought in East Africa August 2022.* (2022).
- 1171 87. Yang, M. *et al.* The role of climate in the trend and variability of Ethiopia's cereal crop
1172 yields. *Sci. Total Environ.* **723**, 137893 (2020).
- 1173 88. Wilkes, M. A. *et al.* Physical and biological controls on fine sediment transport and
1174 storage in rivers. *Wiley Interdisciplinary Reviews: Water* vol. 6 (2019).
- 1175 89. Gebrehiwot, K. A. A review on waterlogging, salinization and drainage in Ethiopian
1176 irrigated agriculture. *Sustain. Water Resour. Manag.* **4**, 55–62 (2018).
- 1177 90. Fenta, A. A. *et al.* Cropland expansion outweighs the monetary effect of declining
1178 natural vegetation on ecosystem services in sub-Saharan Africa. *Ecosyst. Serv.* **45**,
1179 101154 (2020).
- 1180 91. Showler, A. T. Locust 1 (Orthoptera: Acrididae) Outbreak in Africa and Asia, 1992–
1181 1994: An Overview. *Am. Entomol.* (1995) doi:10.1093/ae/41.3.179.
- 1182 92. Foster, Z. J. The 1915 Locust Attack in Syria and Palestine and its Role in the Famine
1183 During the First World War. *Middle East. Stud.* (2015)
1184 doi:10.1080/00263206.2014.976624.
- 1185 93. Showler, A. T. & Potter, C. S. Synopsis of the 1986–1989 Desert Locust (Orthoptera:
1186 Acrididae) Plague and the Concept of Strategic Control. *Am. Entomol.* **37**, (1991).
- 1187 94. Bennett, L. V. The development and termination of the 1968 plague of the desert
1188 locust, *Schistocerca gregaria* (Forskål) (Orthoptera, Acrididae). *Bull. Entomol. Res.*
1189 **66**, (1976).
- 1190 95. Showler, A. T. & Lecoq, M. Incidence and ramifications of armed conflict in countries
1191 with major desert locust breeding areas. *Agronomy* (2021)
1192 doi:10.3390/AGRONOMY11010114.
- 1193 96. IPC. IPC Alert on Locusts by The Integrated Food Security Phase Classification.
1194 (2020).
- 1195 97. Singh, V. K. & Roxy, M. K. A review of ocean-atmosphere interactions during tropical
1196 cyclones in the north Indian Ocean. *Earth-Science Reviews* vol. 226 (2022).
- 1197 98. Yuan, J. P. & Cao, J. North Indian Ocean tropical cyclone activities influenced by the
1198 Indian Ocean Dipole mode. *Sci. China Earth Sci.* **56**, (2013).
- 1199 99. Madani, N. *et al.* Below-surface water mediates the response of African forests to
1200 reduced rainfall. *Environ. Res. Lett.* **15**, (2020).
- 1201 100. Guan, K. *et al.* Photosynthetic seasonality of global tropical forests constrained by
1202 hydroclimate. *Nat. Geosci.* **8**, (2015).
- 1203 101. Madani, N., Kimball, J. S., Jones, L. A., Parazoo, N. C. & Guan, K. Global analysis of
1204 bioclimatic controls on ecosystem productivity using satellite observations of solar-
1205 induced chlorophyll fluorescence. *Remote Sens.* **9**, (2017).
- 1206 102. Schenk, H. J. & Jackson, R. B. Rooting depths, lateral root spreads and below-

- ground/above-ground allometries of plants in water-limited ecosystems. *J. Ecol.* **90**, (2002).
- 1207
1208
- 1209 103. Jones, L. A. *et al.* The SMAP Level 4 Carbon Product for Monitoring Ecosystem Land-
1210 Atmosphere CO₂ Exchange. *IEEE Trans. Geosci. Remote Sens.* **55**, (2017).
- 1211 104. Bauer, S. E., Im, U., Mezuman, K. & Gao, C. Y. Desert Dust, Industrialization, and
1212 Agricultural Fires: Health Impacts of Outdoor Air Pollution in Africa. *J. Geophys. Res.*
1213 *Atmos.* **124**, (2019).
- 1214 105. Jaeglé, L., Steinberger, L., Martin, R. V. & Chance, K. Global partitioning of NO_x
1215 sources using satellite observations: Relative roles of fossil fuel combustion, biomass
1216 burning and soil emissions. in *Faraday Discussions* vol. 130 (2005).
- 1217 106. van der Werf, G. R. *et al.* Global fire emissions estimates during 1997--2016. *Earth*
1218 *Syst. Sci. Data* **9**, 697–720 (2017).
- 1219 107. Bistinas, I., Harrison, S. P., Prentice, I. C. & Pereira, J. M. C. Causal relationships
1220 versus emergent patterns in the global controls of fire frequency. *Biogeosciences* **11**,
1221 (2014).
- 1222 108. Finney, D. L. *et al.* African Lightning and its Relation to Rainfall and Climate Change
1223 in a Convection-Permitting Model. *Geophys. Res. Lett.* **47**, (2020).
- 1224 109. Andela, N. *et al.* A human-driven decline in global burned area. *Science* (80-.). **356**,
1225 (2017).
- 1226 110. Andela, N. & Van Der Werf, G. R. Recent trends in African fires driven by cropland
1227 expansion and El Niño to la Niña transition. *Nat. Clim. Chang.* **4**, (2014).
- 1228 111. Chen, Y. *et al.* A pan-tropical cascade of fire driven by El Niño/Southern Oscillation.
1229 *Nat. Clim. Chang.* **7**, (2017).
- 1230 112. Kim, I. W. *et al.* Tropical Indo-Pacific SST influences on vegetation variability in
1231 eastern Africa. *Sci. Rep.* **11**, (2021).
- 1232 113. Ringeval, B. *et al.* An attempt to quantify the impact of changes in wetland extent on
1233 methane emissions on the seasonal and interannual time scales. *Global Biogeochem.*
1234 *Cycles* (2010) doi:10.1029/2008GB003354.
- 1235 114. Bloom, A. A., Palmer, P. I., Fraser, A., David, S. R. & Frankenberg, C. Large-scale
1236 controls of methanogenesis inferred from methane and gravity spaceborne data.
1237 *Science* (80-.). (2010) doi:10.1126/science.1175176.
- 1238 115. Whalen, S. C. Biogeochemistry of methane exchange between natural wetlands and
1239 the atmosphere. *Environmental Engineering Science* (2005)
1240 doi:10.1089/ees.2005.22.73.
- 1241 116. Bloom, A. A., Palmer, P. I., Fraser, A., Reay, D. S. & Frankenberg, C. Large-Scale
1242 Controls of Methanogenesis Inferred from Methane and Gravity Spaceborne Data.
1243 *Science* (80-.). **327**, 322–325 (2010).
- 1244 117. Helfter, C. *et al.* Phenology is the dominant control of methane emissions in a tropical
1245 non-forested wetland. *Nat. Commun.* **13**, 133 (2022).
- 1246 118. Joabsson, A., Christensen, T. R. & Wallén, B. Vascular plant controls on methane
1247 emissions from northern peatforming wetlands. *Trends in Ecology and Evolution*
1248 (1999) doi:10.1016/S0169-5347(99)01649-3.
- 1249 119. Dingemans, B. J. J., Barker, E. S. & Bodelier, P. L. E. Aquatic herbivores facilitate the
1250 emission of methane from wetlands. *Ecology* (2011) doi:10.1890/10-1297.1.
- 1251 120. Lunt, M. F. *et al.* An increase in methane emissions from tropical Africa between 2010
1252 and 2016 inferred from satellite data. *Atmos. Chem. Phys.* **19**, 14721–14740 (2019).
- 1253 121. Lunt, M. F. *et al.* Rain-fed pulses of methane from East Africa during 2018-2019
1254 contributed to atmospheric growth rate. *Environ. Res. Lett.* **16**, 24021 (2021).
- 1255 122. Pandey, S. *et al.* Using satellite data to identify the methane emission controls of
1256 South Sudan's wetlands. *Biogeosciences* (2021) doi:10.5194/bg-18-557-2021.
- 1257 123. Feng, L., Palmer, P. I., Zhu, S., Parker, R. J. & Liu, Y. Tropical methane emissions
1258 explain large fraction of recent changes in global atmospheric methane growth rate.
1259 *Nat. Commun.* **13**, 1378 (2022).
- 1260 124. Sutcliffe, J. V. & Parks, Y. P. *The hydrology of the Nile. The hydrology of the Nile.*
1261 *IAHS Special Publication No.5.* (1999).

- 1262 125. Sutcliffe, J. & Brown, E. Water losses from the Sudd. *Hydrol. Sci. J.* (2018)
1263 doi:10.1080/02626667.2018.1438612.
- 1264 126. Lunt, M. F. *et al.* Rain-fed pulses of methane from East Africa during 2018-2019
1265 contributed to atmospheric growth rate. *Environ. Res. Lett.* **16**, 24021 (2021).
- 1266 127. Qu, Z. *et al.* Attribution of the 2020 surge in atmospheric methane by inverse analysis
1267 of GOSAT observations. *Environ. Res. Lett.* **17**, 094003 (2022).
- 1268 128. Feng, L., Palmer, P. I., Parker, R. J., Lunt, M. F. & Boesch, H. Methane emissions
1269 responsible for record-breaking atmospheric methane growth rates in 2020 and 2021.
1270 *Atmos. Chem. Phys. Discuss.* **2022**, 1–23 (2022).
- 1271 129. Van Damme, M. *et al.* Industrial and agricultural ammonia point sources exposed.
1272 *Nature* **564**, (2018).
- 1273 130. Dammers, E. *et al.* NH₃ emissions from large point sources derived from CrIS and
1274 IASI satellite observations. *Atmos. Chem. Phys.* **19**, (2019).
- 1275 131. Bauer, S. E., Tsigaridis, K. & Miller, R. Significant atmospheric aerosol pollution
1276 caused by world food cultivation. *Geophys. Res. Lett.* **43**, (2016).
- 1277 132. Lelieveld, J., Evans, J. S., Fnais, M., Giannadaki, D. & Pozzer, A. The contribution of
1278 outdoor air pollution sources to premature mortality on a global scale. *Nature* **525**,
1279 (2015).
- 1280 133. Denier Van Der Gon, H. & Bleeker, A. Indirect N₂O emission due to atmospheric N
1281 deposition for the Netherlands. *Atmos. Environ.* **39**, (2005).
- 1282 134. Krupa, S. V. Effects of atmospheric ammonia (NH₃) on terrestrial vegetation: A
1283 review. *Environmental Pollution* vol. 124 (2003).
- 1284 135. Matson, P. A., McDowell, W. H., Townsend, A. R. & Vitousek, P. M. The globalization
1285 of N deposition: Ecosystem consequences in tropical environments. *Biogeochemistry*
1286 **46**, (1999).
- 1287 136. Tian, D. & Niu, S. A global analysis of soil acidification caused by nitrogen addition.
1288 *Environ. Res. Lett.* **10**, (2015).
- 1289 137. Koutsoyiannis, D., Yao, H. & Georgakakos, A. Medium-range flow prediction for the
1290 Nile: a comparison of stochastic and deterministic methods / Prévision du débit du Nil
1291 à moyen terme: une comparaison de méthodes stochastiques et déterministes.
1292 *Hydrol. Sci. J.* **53**, 142–164 (2008).
- 1293 138. Kim, M. & Or, D. Microscale pH variations during drying of soils and desert biocrusts
1294 affect HONO and NH₃ emissions. *Nat. Commun.* **10**, (2019).
- 1295 139. Roelle, P. A. & Aneja, V. P. Characterization of ammonia emissions from soils in the
1296 upper coastal plain, North Carolina. *Atmos. Environ.* **36**, (2002).
- 1297 140. Clarisse, L. *et al.* Atmospheric ammonia (NH₃) emanations from Lake Natron's
1298 saline mudflats. *Sci. Rep.* **9**, (2019).
- 1299 141. Hickman, J. E. *et al.* Changes in biomass burning, wetland extent, or agriculture drive
1300 atmospheric NH₃ trends in select African regions. *Atmos. Chem. Phys.* **21**, (2021).
- 1301 142. Di Vittorio, C. A. & Georgakakos, A. P. Land cover classification and wetland
1302 inundation mapping using MODIS. *Remote Sens. Environ.* **204**, (2018).
- 1303 143. Oluwasanya, G. . P. D. . Q. M. . S. V. *Water Security in Africa: A Preliminary*
1304 *Assessment* . (2022).
- 1305 144. Sridharan, V. *et al.* Resilience of the Eastern African electricity sector to climate driven
1306 changes in hydropower generation. *Nat. Commun.* **10**, 302 (2019).
- 1307 145. Jeuland, M. Economic implications of climate change for infrastructure planning in
1308 transboundary water systems: An example from the Blue Nile. *Water Resour. Res.*
1309 **46**, W11556 (2010).
- 1310 146. Jeuland, M. & Whittington, D. Water resources planning under climate change:
1311 Assessing the robustness of real options for the Blue Nile. *Water Resour. Res.* **50**,
1312 2086–2107 (2014).
- 1313 147. Conway, D. Water resources: Future Nile river flows. *Nat. Clim. Chang.* **7**, 319–320
1314 (2017).
- 1315 148. Siderius, C. *et al.* Hydrological Response and Complex Impact Pathways of the
1316 2015/2016 El Niño in Eastern and Southern Africa. *Earth's Futur.* **6**, (2018).

- 1317 149. Samboko, P. *et al.* The Impact of Power Rationing on Zambia's Agricultural Sector.
1318 *Work. Pap. No. 105* (2016).
- 1319 150. Dinar, A., Blankespoor, B., Dinar, S. & Kurukulasuriya, P. Does precipitation and
1320 runoff variability affect treaty cooperation between states sharing international bilateral
1321 rivers? *Ecol. Econ.* **69**, 2568–2581 (2010).
- 1322 151. Wheeler, K. G., Jeuland, M., Hall, J. W., Zagona, E. & Whittington, D. Understanding
1323 and managing new risks on the Nile with the Grand Ethiopian Renaissance Dam. *Nat.*
1324 *Commun.* **11**, 5222 (2020).
- 1325 152. Peña-Ramos, J. A., José López-Bedmar, R., Sastre, F. J. & Martínez-Martínez, A.
1326 Water Conflicts in Sub-Saharan Africa. *Front. Environ. Sci.* **10**, (2022).
- 1327 153. Wolf, A. T. Shared Waters: Conflict and Cooperation. *Annu. Rev. Environ. Resour.* **32**,
1328 241–269 (2007).
- 1329 154. Calderón, C. & Servén, L. Infrastructure and Economic Development in Sub-Saharan
1330 Africa †. *J. Afr. Econ.* **19**, i13–i87 (2010).
- 1331 155. Douglas, I. *et al.* Unjust waters: climate change, flooding and the urban poor in Africa.
1332 *Environ. Urban.* **20**, 187–205 (2008).
- 1333 156. Birhanu, D., Kim, H., Jang, C. & Park, S. Flood Risk and Vulnerability of Addis Ababa
1334 City Due to Climate Change and Urbanization. *Procedia Eng.* **154**, 696–702 (2016).
- 1335 157. Mahmood, M. I., Elagib, N. A., Horn, F. & Saad, S. A. G. Lessons learned from
1336 Khartoum flash flood impacts: An integrated assessment. *Sci. Total Environ.* **601–**
1337 **602**, 1031–1045 (2017).
- 1338 158. AFB. Flooding: Sudan. *Africa Res. Bull. Econ. Financ. Tech. Ser.* **57**, 23103A-23106C
1339 (2020).
- 1340 159. Thomson, M. C., Muñoz, Á. G., Cousin, R. & Shumake-Guillemot, J. Climate drivers
1341 of vector-borne diseases in Africa and their relevance to control programmes. *Infect.*
1342 *Dis. Poverty* (2018) doi:10.1186/s40249-018-0460-1.
- 1343 160. Caminade, C., McIntyre, K. M. & Jones, A. E. Impact of recent and future climate
1344 change on vector-borne diseases. *Annals of the New York Academy of Sciences*
1345 (2019) doi:10.1111/nyas.13950.
- 1346 161. Endo, N. & Eltahir, E. A. B. Increased risk of malaria transmission with warming
1347 temperature in the Ethiopian Highlands. *Environ. Res. Lett.* **15**, 54006 (2020).
- 1348 162. Brown, V., Issak, M. A., Rossi, M., Barboza, P. & Paugam, A. Epidemic of malaria in
1349 north-eastern Kenya. *Lancet* (1998) doi:10.1016/S0140-6736(05)60747-7.
- 1350 163. Kilian, A. H. D., Langi, P., Talisuna, A. & Kabagambe, G. Rainfall pattern, El Nino and
1351 malaria in Uganda. *Trans. R. Soc. Trop. Med. Hyg.* (1999) doi:10.1016/S0035-
1352 9203(99)90165-7.
- 1353 164. Boyce, R. *et al.* Severe Flooding and Malaria Transmission in the Western Ugandan
1354 Highlands: Implications for Disease Control in an Era of Global Climate Change. *J.*
1355 *Infect. Dis.* (2016) doi:10.1093/infdis/jiw363.
- 1356 165. Nosrat, C. *et al.* Impact of recent climate extremes on mosquito-borne disease
1357 transmission in kenya. *PLoS Negl. Trop. Dis.* (2021)
1358 doi:10.1371/journal.pntd.0009182.
- 1359 166. Hashizume, M., Terao, T. & Minakawa, N. The Indian Ocean Dipole and malaria risk
1360 in the highlands of western Kenya. *Proc. Natl. Acad. Sci. U. S. A.* (2009)
1361 doi:10.1073/pnas.0806544106.
- 1362 167. Hashizume, M., Chaves, L. F. & Minakawa, N. Indian Ocean Dipole drives malaria
1363 resurgence in East African highlands. *Sci. Rep.* (2012) doi:10.1038/srep00269.
- 1364 168. Moore, S. M. *et al.* El Niño and the shifting geography of cholera in Africa. *Proc. Natl.*
1365 *Acad. Sci. U. S. A.* (2017) doi:10.1073/pnas.1617218114.
- 1366 169. Rieckmann, A., Tamason, C. C., Gurley, E. S., Rod, N. H. & Jensen, P. K. M.
1367 Exploring droughts and floods and their association with cholera outbreaks in sub-
1368 saharan africa: a register-based ecological study from 1990 to 2010. *Am. J. Trop.*
1369 *Med. Hyg.* (2018) doi:10.4269/ajtmh.17-0778.
- 1370 170. Lindsay, S. W., Bødker, R., Malima, R., Msangeni, H. A. & Kisinza, W. Effect of 1997-
1371 98 El Nino on highland malaria in Tanzania. *Lancet* (2000) doi:10.1016/S0140-

- 1372 6736(00)90022-9.
- 1373 171. Chemura, A., Mudereri, B. T., Yalew, A. W. & Gornott, C. Climate change and
1374 specialty coffee potential in Ethiopia. *Sci. Rep.* **11**, (2021).
- 1375 172. Lobell, D. B. & Burke, M. B. Why are agricultural impacts of climate change so
1376 uncertain? the importance of temperature relative to precipitation. *Environ. Res. Lett.*
1377 **3**, (2008).
- 1378 173. Tigchelaar, M., Battisti, D. S., Naylor, R. L. & Ray, D. K. Future warming increases
1379 probability of globally synchronized maize production shocks. *Proc. Natl. Acad. Sci. U.*
1380 *S. A.* **115**, (2018).
- 1381 174. Shapiro, L. L. M., Whitehead, S. A. & Thomas, M. B. Quantifying the effects of
1382 temperature on mosquito and parasite traits that determine the transmission potential
1383 of human malaria. *PLoS Biol.* **15**, (2017).
- 1384 175. Yang, W., Seager, R., Cane, M. A. & Lyon, B. The East African long rains in
1385 observations and models. *J. Clim.* **27**, (2014).
- 1386 176. Rowell, D. P., Booth, B. B. B., Nicholson, S. E. & Good, P. Reconciling past and
1387 future rainfall trends over East Africa. *J. Clim.* **28**, (2015).
- 1388 177. Dunning, C. M., Black, E. & Allan, R. P. Later Wet Seasons with More Intense Rainfall
1389 over Africa under Future Climate Change. *J. Clim.* **31**, 9719–9738 (2018).
- 1390 178. Makula, E. K. & Zhou, B. Coupled Model Intercomparison Project phase 6 evaluation
1391 and projection of East African precipitation. *Int. J. Climatol.* (2021)
1392 doi:10.1002/joc.7373.
- 1393 179. Cook, B. I. *et al.* Twenty-First Century Drought Projections in the CMIP6 Forcing
1394 Scenarios. *Earth's Futur.* **8**, (2020).
- 1395 180. Ongoma, V., Chena, H. & Gaoa, C. Projected changes in mean rainfall and
1396 temperature over east Africa based on CMIP5 models. *Int. J. Climatol.* **38**, (2018).
- 1397 181. Akinsanola, A. A., Ongoma, V. & Kooperman, G. J. Evaluation of CMIP6 models in
1398 simulating the statistics of extreme precipitation over Eastern Africa. *Atmos. Res.* **254**,
1399 (2021).
- 1400 182. Rowell, D. P., Senior, C. A., Vellinga, M. & Graham, R. J. Can climate projection
1401 uncertainty be constrained over Africa using metrics of contemporary performance?
1402 *Clim. Change* **134**, (2016).
- 1403 183. Endris, H. S. *et al.* Future changes in rainfall associated with ENSO, IOD and
1404 changes in the mean state over Eastern Africa. *Clim. Dyn.* **52**, (2019).
- 1405 184. Ayugi, B. *et al.* Comparison of CMIP6 and CMIP5 models in simulating mean and
1406 extreme precipitation over East Africa. *Int. J. Climatol.* **41**, (2021).
- 1407 185. Iturbide, M. *et al.* Repository supporting the implementation of FAIR principles in the
1408 IPCC-WG1 Atlas. (2021) doi:10.5281/zenodo.3691645.
- 1409 186. Finney, D. L. *et al.* Effects of Explicit Convection on Future Projections of Mesoscale
1410 Circulations, Rainfall, and Rainfall Extremes over Eastern Africa. *J. Clim.* **33**, 2701–
1411 2718 (2020).
- 1412 187. Lyon, B. Biases in sea surface temperature and the annual cycle of Greater Horn of
1413 Africa rainfall in CMIP6. *Int. J. Climatol.* (2021) doi:10.1002/joc.7456.
- 1414 188. King, J. A., Washington, R. & Engelstaedter, S. Representation of the Indian Ocean
1415 Walker circulation in climate models and links to Kenyan rainfall. *Int. J. Climatol.* **41**,
1416 (2021).
- 1417 189. Cai, W. *et al.* Changing El Niño–Southern Oscillation in a warming climate. *Nature*
1418 *Reviews Earth and Environment* vol. 2 (2021).
- 1419 190. Zelle, H., van Oldenborgh, G. J., Burgers, G. & Dijkstra, H. El Niño and greenhouse
1420 warming: Results from ensemble simulations with the NCAR CCSM. *J. Clim.* **18**,
1421 (2005).
- 1422 191. Merryfield, W. J. Changes to ENSO under CO2 doubling in a multimodel ensemble. *J.*
1423 *Clim.* **19**, (2006).
- 1424 192. Collins, M. *et al.* The impact of global warming on the tropical Pacific Ocean and El
1425 Niño. *Nat. Geosci.* **3**, (2010).
- 1426 193. Cai, W. *et al.* Increasing frequency of extreme El Niño events due to greenhouse

- 1427 warming. *Nat. Clim. Chang.* **4**, (2014).
- 1428 194. Cai, W. *et al.* ENSO and greenhouse warming. *Nature Climate Change* vol. 5 (2015).
- 1429 195. Singh, J. *et al.* Enhanced risk of concurrent regional droughts with increased ENSO
1430 variability and warming. *Nat. Clim. Chang.* **12**, 163–170 (2022).
- 1431 196. Zheng, X. T. *et al.* Indian ocean dipole response to global warming in the CMIP5
1432 multimodel ensemble. *J. Clim.* **26**, (2013).
- 1433 197. Cai, W. & Cowan, T. Why is the amplitude of the Indian ocean dipole overly large in
1434 CMIP3 and CMIP5 climate models? *Geophys. Res. Lett.* **40**, (2013).
- 1435 198. Cai, W. *et al.* Opposite response of strong and moderate positive Indian Ocean Dipole
1436 to global warming. *Nat. Clim. Chang.* **11**, (2021).
- 1437 199. Douville, H. *et al.* Climate Change 2021: The Physical Science Basis. Contribution of
1438 Working Group I to the Sixth Assessment Report of the Intergovernmental Panel on
1439 Climate Change. in (Cambridge University Press, 2021).
- 1440 200. Chu, J. E. *et al.* Future change of the Indian Ocean basin-wide and dipole modes in
1441 the CMIP5. *Clim. Dyn.* **43**, (2014).
- 1442 201. Mamalakis, A. *et al.* Zonally contrasting shifts of the tropical rain belt in response to
1443 climate change. *Nat. Clim. Chang.* **11**, (2021).
- 1444 202. Schlenker, W. & Roberts, M. J. Nonlinear temperature effects indicate severe
1445 damages to U.S. crop yields under climate change. *Proc. Natl. Acad. Sci. U. S. A.*
1446 **106**, (2009).
- 1447 203. Wang, X., Xie, H., Guan, H. & Zhou, X. Different responses of MODIS-derived NDVI
1448 to root-zone soil moisture in semi-arid and humid regions. *J. Hydrol.* **340**, (2007).
- 1449 204. Guido, Z. *et al.* Farmer forecasts: Impacts of seasonal rainfall expectations on
1450 agricultural decision-making in Sub-Saharan Africa. *Clim. Risk Manag.* **30**, (2020).
- 1451 205. Thornton, P. K., van de Steeg, J., Notenbaert, A. & Herrero, M. The impacts of climate
1452 change on livestock and livestock systems in developing countries: A review of what
1453 we know and what we need to know. *Agricultural Systems* vol. 101 (2009).
- 1454 206. Senande-Rivera, M., Insua-Costa, D. & Miguez-Macho, G. Spatial and temporal
1455 expansion of global wildland fire activity in response to climate change. *Nat. Commun.*
1456 **13**, 1208 (2022).
- 1457 207. Piao, S. *et al.* Characteristics, drivers and feedbacks of global greening. *Nature*
1458 *Reviews Earth and Environment* vol. 1 (2020).
- 1459 208. Zarei, A., Chemura, A., Gleixner, S. & Hoff, H. Evaluating the grassland NPP
1460 dynamics in response to climate change in Tanzania. *Ecol. Indic.* **125**, (2021).
- 1461 209. Martens, C. *et al.* Large uncertainties in future biome changes in Africa call for flexible
1462 climate adaptation strategies. *Glob. Chang. Biol.* **27**, (2021).
- 1463 210. Doherty, R. M., Sitch, S., Smith, B., Lewis, S. L. & Thornton, P. K. Implications of
1464 future climate and atmospheric CO₂ content for regional biogeochemistry,
1465 biogeography and ecosystem services across East Africa. *Glob. Chang. Biol.* **16**,
1466 (2010).
- 1467 211. Scheiter, S. & Higgins, S. I. Impacts of climate change on the vegetation of Africa: An
1468 adaptive dynamic vegetation modelling approach. *Glob. Chang. Biol.* **15**, (2009).
- 1469 212. Kim, J. H. *et al.* A Systematic Review of Typhoid Fever Occurrence in Africa. *Clinical*
1470 *Infectious Diseases* vol. 69 (2019).
- 1471 213. Lahondre, C. & Lazzari, C. R. Mosquitoes cool down during blood feeding to avoid
1472 overheating. *Curr. Biol.* **22**, (2012).
- 1473 214. Colón-González, F. J. *et al.* Projecting the risk of mosquito-borne diseases in a
1474 warmer and more populated world: a multi-model, multi-scenario intercomparison
1475 modelling study. *Lancet Planet. Heal.* **5**, (2021).
- 1476 215. Ryan, S. J., Lippi, C. A. & Zermoglio, F. Shifting transmission risk for malaria in Africa
1477 with climate change: A framework for planning and intervention. *Malar. J.* **19**, (2020).
- 1478 216. Kolstad, E. W., MacLeod, D. & Demissie, T. D. Drivers of Subseasonal Forecast
1479 Errors of the East African Short Rains. *Geophys. Res. Lett.* **48**, (2021).
- 1480 217. Ogutu, G. E. O., Franssen, W. H. P., Supit, I., Omondi, P. & Hutjes, R. W. A. Skill of
1481 ECMWF system-4 ensemble seasonal climate forecasts for East Africa. *Int. J.*

- 1482 *Climatol.* **37**, (2017).
- 1483 218. Young, H. R. & Klingaman, N. P. Skill of seasonal rainfall and temperature forecasts
1484 for East Africa. *Weather Forecast.* **35**, (2020).
- 1485 219. Funk, C. *et al.* Predicting East African spring droughts using Pacific and Indian Ocean
1486 sea surface temperature indices. *Hydrol. Earth Syst. Sci.* **18**, (2014).
- 1487 220. Mutai, C. C., Ward, M. N. & Colman, A. W. Towards the prediction of the East Africa
1488 short rains based on sea-surface temperature-atmosphere coupling. *Int. J. Climatol.*
1489 **18**, (1998).
- 1490 221. Nicholson, S. E. The predictability of rainfall over the greater horn of Africa. Part I:
1491 Prediction of seasonal rainfall. *J. Hydrometeorol.* **15**, (2014).
- 1492 222. Meehl, G. A. *et al.* Initialized Earth System prediction from subseasonal to decadal
1493 timescales. *Nature Reviews Earth and Environment* vol. 2 (2021).
- 1494 223. MacLeod, D. Seasonal forecasts of the East African long rains: insight from
1495 atmospheric relaxation experiments. *Clim. Dyn.* **53**, (2019).
- 1496 224. Phillips, H. E. *et al.* Progress in understanding of Indian Ocean circulation, variability,
1497 air-sea exchange, and impacts on biogeochemistry. *Ocean Science* vol. 17 (2021).
- 1498 225. Majumdar, S. J. A review of targeted observations. *Bulletin of the American*
1499 *Meteorological Society* vol. 97 (2016).
- 1500 226. Dong, B., Haines, K. & Martin, M. Improved High Resolution Ocean Reanalyses Using
1501 a Simple Smoother Algorithm. *J. Adv. Model. Earth Syst.* **13**, (2021).
- 1502 227. Smith, M. J. *et al.* Changing how earth system modeling is done to provide more
1503 useful information for decision making, science, and society. *Bulletin of the American*
1504 *Meteorological Society* vol. 95 (2014).
- 1505 228. Webster, P. J. Meteorology: Improve weather forecasts for the developing world.
1506 *Nature* vol. 493 (2013).
- 1507 229. Mordecai, E. A., Ryan, S. J., Caldwell, J. M., Shah, M. M. & LaBeaud, A. D. Climate
1508 change could shift disease burden from malaria to arboviruses in Africa. *Lancet*
1509 *Planet. Heal.* **4**, e416–e423 (2020).
- 1510 230. Allen, T. *et al.* Global hotspots and correlates of emerging zoonotic diseases. *Nat.*
1511 *Commun.* **8**, (2017).
- 1512 231. Lipp, E. K., Huq, A. & Colwell, R. R. Effects of global climate on infectious disease:
1513 The cholera model. *Clinical Microbiology Reviews* vol. 15 (2002).
- 1514 232. Tamerius, J. D. *et al.* Environmental Predictors of Seasonal Influenza Epidemics
1515 across Temperate and Tropical Climates. *PLoS Pathog.* **9**, (2013).
- 1516 233. Palmer, P. I. *et al.* Net carbon emissions from African biosphere dominate pan-tropical
1517 atmospheric CO₂ signal. *Nat. Commun.* **10**, 3344 (2019).
- 1518 234. Merbold, L. *et al.* Opportunities for an African greenhouse gas observation system.
1519 *Reg. Environ. Chang.* **21**, (2021).
- 1520 235. Wang, T. *et al.* Why is the Indo-Gangetic Plain the region with the largest NH 3
1521 column in the globe during pre-monsoon and monsoon seasons? *Atmos. Chem.*
1522 *Phys.* **20**, 8727–8736 (2020).
- 1523 236. Cai, W. *et al.* Projected response of the Indian Ocean Dipole to greenhouse warming.
1524 *Nature Geoscience* vol. 6 (2013).
- 1525 237. Tramberend, S. *et al.* Co-development of East African regional water scenarios for
1526 2050. *One Earth* **4**, (2021).
- 1527 238. Zhao, G., Li, Y., Zhou, L. & Gao, H. Evaporative water loss of 1.42 million global
1528 lakes. *Nat. Commun.* **13**, 3686 (2022).
- 1529 239. Haghghi, E., Madani, K. & Hoekstra, A. Y. The water footprint of water conservation
1530 using shade balls in California. *Nat. Sustain.* **1**, (2018).
- 1531 240. FAO and UN Water. *Progress on change in water-use efficiency. Global status and*
1532 *acceleration needs for SDG indicator 6.4.1.* (2021).
- 1533 241. Acreman, M. C. *et al.* Managed flood releases from reservoirs: issues and guidance.
1534 *Rep. to DFID World Comm. Dams. Cent. Ecol. Hydrol. Wallingford, UK 2000*, p86
1535 (2000).
- 1536 242. Wang, J. *et al.* Exploitation of drought tolerance-related genes for crop improvement.

- 1537 *International Journal of Molecular Sciences* vol. 22 (2021).
- 1538 243. Biamah, E. K., Gichuki, F. N. & Kaumbutho, P. G. Tillage methods and soil and water
1539 conservation in eastern Africa. *Soil Tillage Res.* **27**, (1993).
- 1540 244. Parncutt, R. The human cost of anthropogenic global warming: Semi-quantitative
1541 prediction and the 1,000-tonne rule. *Front. Psychol.* **10**, (2019).
- 1542 245. Schreck, C. J. & Semazzi, F. H. M. Variability of the recent climate of eastern Africa.
1543 *Int. J. Climatol.* **24**, 681–701 (2004).
- 1544 246. Sutcliffe, J. & Parks, Y. *The hydrology of the Nile*. (IAHS Press, 1999).
- 1545 247. Alsdorf, D. *et al.* Opportunities for hydrologic research in the Congo Basin. *Reviews of*
1546 *Geophysics* vol. 54 (2016).
- 1547 248. Lehner, B. & Grill, G. Global river hydrography and network routing: Baseline data and
1548 new approaches to study the world's large river systems. *Hydrol. Process.* **27**, (2013).
- 1549 249. Becker, A. *et al.* A description of the global land-surface precipitation data products of
1550 the Global Precipitation Climatology Centre with sample applications including
1551 centennial (trend) analysis from 1901-present. *Earth Syst. Sci. Data* **5**, (2013).
- 1552 250. Schneider, U. *et al.* GPCP's new land surface precipitation climatology based on
1553 quality-controlled in situ data and its role in quantifying the global water cycle. *Theor.*
1554 *Appl. Climatol.* **115**, (2014).
- 1555 251. Funk, C. *et al.* The climate hazards infrared precipitation with stations - A new
1556 environmental record for monitoring extremes. *Sci. Data* **2**, (2015).
- 1557 252. Gedney, N., Huntingford, C., Comyn-Platt, E. & Wiltshire, A. Significant feedbacks of
1558 wetland methane release on climate change and the causes of their uncertainty.
1559 *Environ. Res. Lett.* **14**, (2019).
- 1560 253. Best, M. J. *et al.* The Joint UK Land Environment Simulator (JULES), model
1561 description – Part 1: Energy and water fluxes. *Geosci. Model Dev.* **4**, (2011).
- 1562 254. Clark, D. B. *et al.* The Joint UK Land Environment Simulator (JULES), model
1563 description – Part 2: Carbon fluxes and vegetation dynamics. *Geosci. Model Dev.* **4**,
1564 (2011).
- 1565 255. Huntingford, C. *et al.* IMOGEN: An intermediate complexity model to evaluate
1566 terrestrial impacts of a changing climate. *Geosci. Model Dev.* **3**, (2010).
- 1567 256. Huntingford, C. & Cox, P. M. An analogue model to derive additional climate change
1568 scenarios from existing GCM simulations. *Clim. Dyn.* **16**, (2000).
- 1569
- 1570
- 1571

1572 **BOX 1: Physical geography of Eastern Africa**

1573

1574 The physical geography of Eastern Africa is relevant to the dynamics of rainfall weather
1575 systems^{47,245} and to the subsequent surface movement of water (see figure). The region is
1576 dominated by the East African Rift, running from the Afar Triple Junction near the Red Sea
1577 southwards through East Africa to Mozambique that also produces the Ethiopian and Kenyan
1578 Highlands.

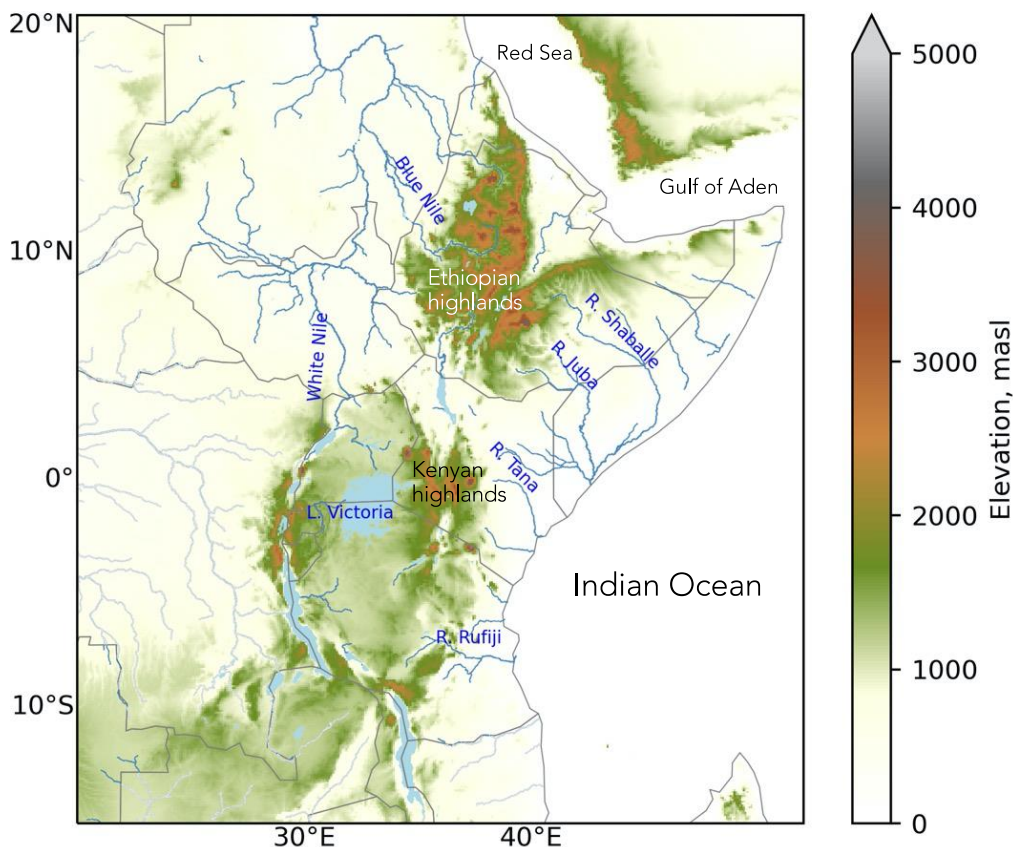
1579

1580 Eastern Africa is dominated by the Nile River basin but also encompasses tributaries of the
1581 Congo as well several regionally important rivers draining eastwards into the Red Sea, the
1582 Gulf of Aden and the Indian Ocean. Two endorheic rivers, the Awash and Omo, terminate in
1583 the Afar depression and Lake Turkana, respectively. The Nile Basin includes several rift valley
1584 lakes including Lake Victoria which collects water from Burundi, Rwanda, northern Tanzania,
1585 and the Kenyan Highlands and has an important role in regulating flows in the White Nile
1586 downstream.

1587

1588 Tributaries draining the western Ethiopian highlands bring additional seasonal flows (during
1589 August-October) with the largest of these, the Blue Nile, joining at Khartoum to form the main
1590 river Nile²⁴⁶. Lake Kivu and Lake Tanganyika and its tributaries in western Tanzania form the
1591 headwaters of the Congo²⁴⁷. Watersheds east and south of the Ethiopian highlands and
1592 eastern rift valley flow into the Indian Ocean, providing an essential source of water to
1593 populations in more arid coastal plains, for example Shabelle and Juba in Somalia. In addition
1594 to the rift valley lakes, areas of extensive seasonal flooding, for example the Sudd in South
1595 Sudan, lead to significant water losses to the atmosphere by evaporation¹²⁵.

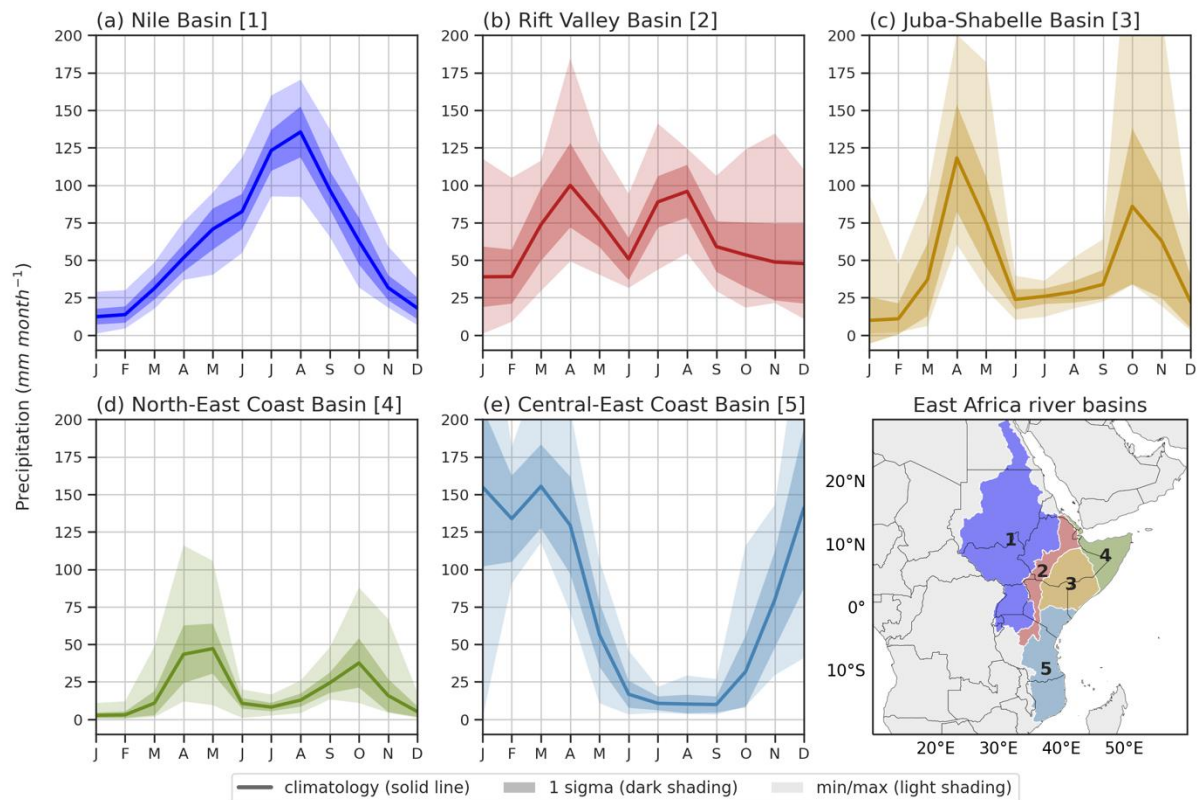
1596



1597

1598

Figure

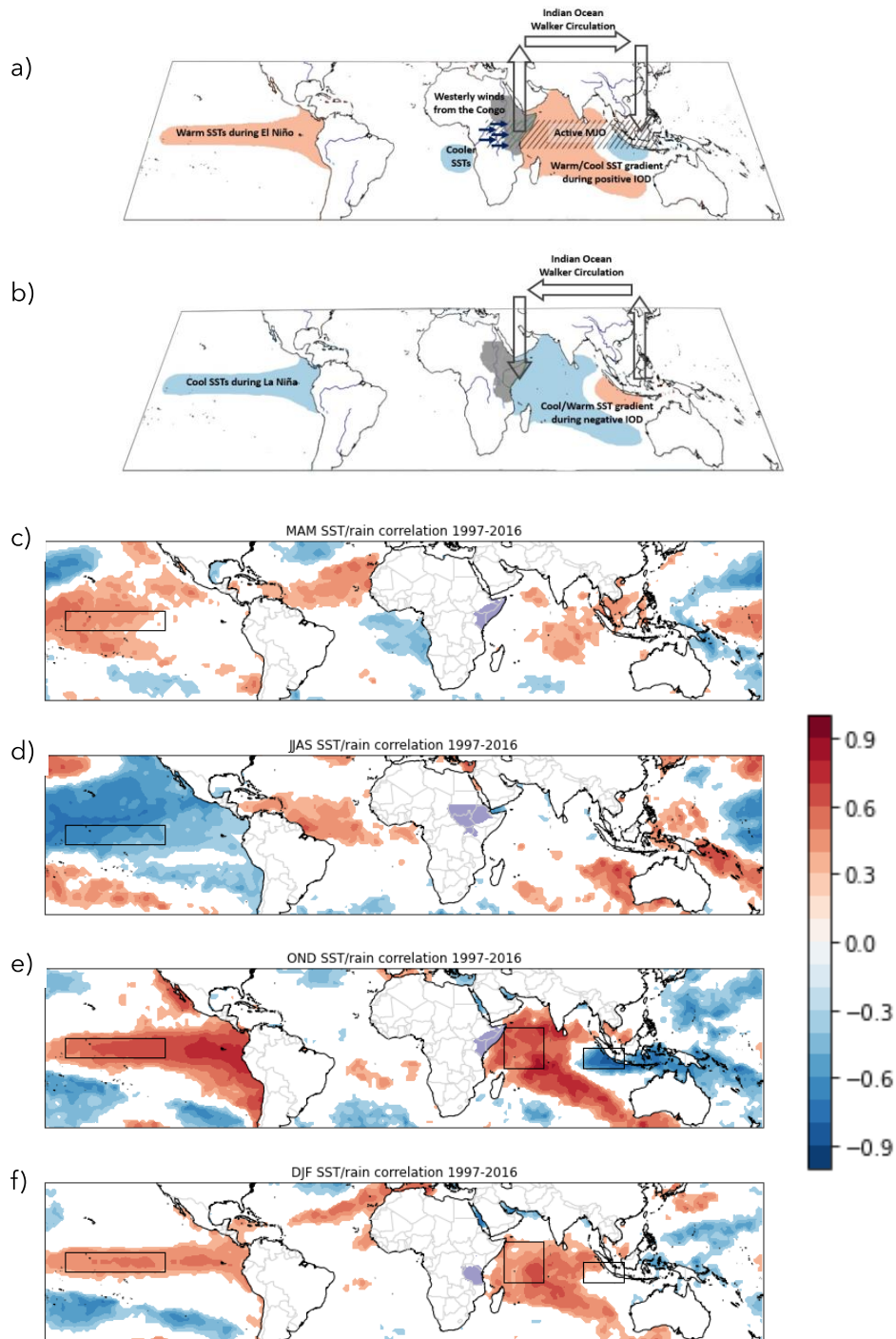


1600

1601 **Figure 1 Seasonal cycle of rainfall, across five river basins (a-e) across Eastern Africa**
 1602 **(f), 1983-2019. a]** Mean seasonal rainfall in the Nile Basin (area 1 in the map, as delineated
 1603 by HydroBASINS²⁴⁸). The dark blue envelope denotes the standard deviation about the
 1604 monthly mean values and the light blue envelope the range of values. Values are calculated
 1605 from the monthly gridded gauge data from the Global Precipitation Climatology Centre
 1606 (GPCC)^{249,250}. **b]** As in a, but for the Rift Valley Basin (area 2 in the map). **c]** As in a, but for
 1607 the Juba-Shabelle Basin (area 3 in the map). **d]** As in a, but for the North-East Coast Basin
 1608 (area 4 in the map). **e]** As in a, but for the Central-East Coast Basin (area 5 in the map).
 1609 Substantial differences in the magnitude, variation and (bimodal) seasonal cycle of rainfall are
 1610 evident across Eastern Africa.

1611

1612



1613

1614

1615

1616

1617

1618

1619

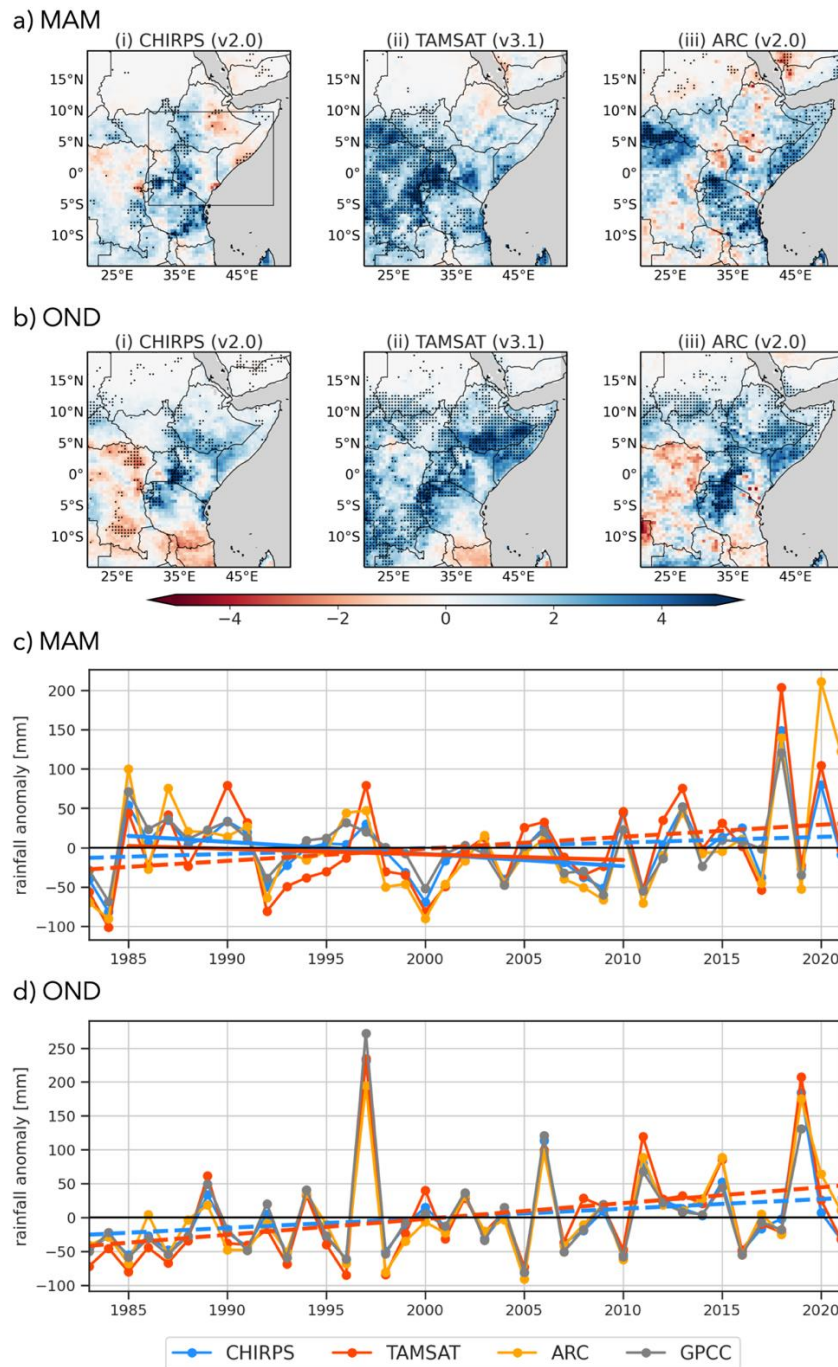
1620

1621

1622

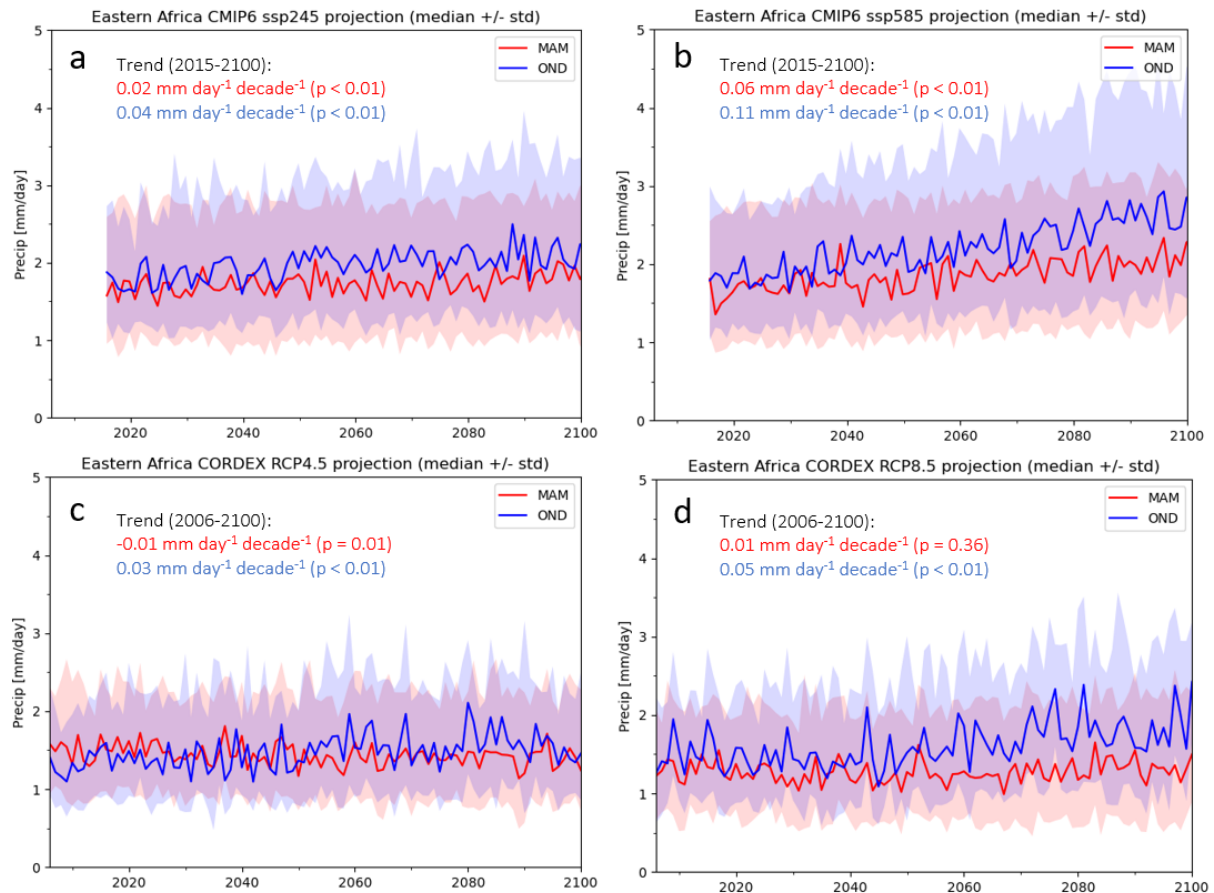
1623

Figure 2 the main physical processes that determine rainfall variations over Eastern Africa. a) mechanisms that lead to enhanced rainfall over Eastern Africa. Orange and blue shading denotes warm and cool sea surface temperatures (SSTs), respectively b) Mechanisms that lead to reduced rainfall over Eastern Africa during La Niña and/or negative Indian Ocean Dipole phases. Rainfall variations are determined by processes that act on local spatial scales and via atmospheric teleconnections. The green contour marks the region that experiences a bimodal regime. c-f) seasonal correlations between SST and regional East African rainfall (denoted by areas with purple shading. Black open rectangles over the Pacific and Indian Ocean define the regions we use to calculate the ENSO and IOD.



1624
 1625
 1626
 1627
 1628
 1629
 1630
 1631
 1632
 1633
 1634
 1635
 1636

Figure 3 Spatial and temporal variations of rainfall over Eastern Africa. **a)** mean rainfall trends during the long rains (MAM) over 1983-2021 for four datasets: CHIRPS²⁵¹ (top left); TAMSAT³⁸ (top right); ARC⁸² (bottom left); and the GPCP²⁴⁹ (bottom right). Stippling denotes statistically significant trends at the 95% confidence level using the Wald test. **b)** as in a, but for the short rain (OND). **c)** area-weighted total rainfall anomalies during MAM over part of Eastern Africa (30-50°E, 5°S-10°N; see box in top left panel of a) for the four datasets. Anomalies are calculated relative to the 1983-2021 monthly means. **d)** As in c, but for OND. Dashed and solid lines denote linear trend lines for CHIRPS and TAMSAT over periods 1983-2021 and 1985-2010, respectively, with colours corresponding to the data; the shorter period is used to highlight changes in the long rains in the 1990s. There is better agreement between trends determined by different rainfall data products for the short rains.



1637

1638

1639

1640

1641

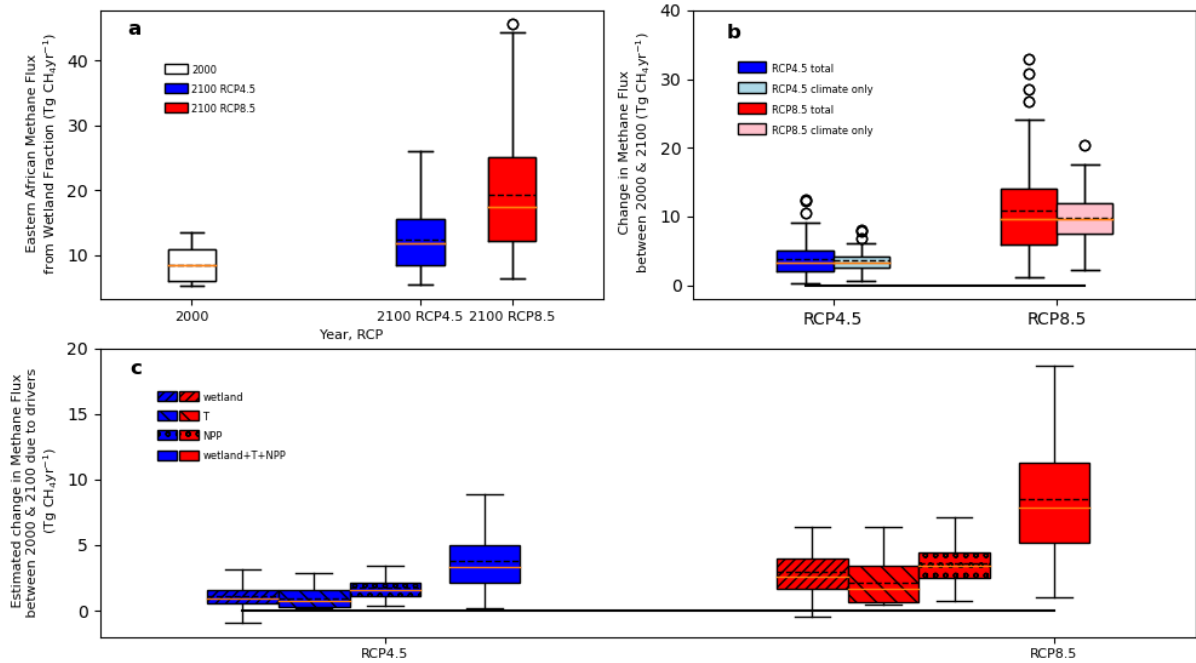
1642

1643

1644

1645

Figure 4 Projections of long rains and short rains. **a)** Multi-model median long rain (MAM; red) and short rain (OND; blue) projections from CMIP6 models forced under SSP 2-4.5. Shading denotes the standard deviation associated with the ensemble of model runs. **b)** As in a, but for CMIP6 models forced under SSP 5-8.5. **c)** Multi-model median long rain (MAM; red) and short rain (OND; blue) projections from CORDEX regional climate models forced with RCP4.5. **d)** As in c, but for CORDEX regional climate forced with RCP8.5. Global and regional climate model projections suggest that short rain totals will exceed those of the long rains, the timing of which depends on the future scenario.



1646

1647

1648

1649

1650

1651

1652

1653

1654

1655

1656

1657

1658

Figure 5 Wetland methane emission over Eastern. **a**] methane emission estimates from the JULES model for 2000 (white) and 2100 driven by RCP4.5 (blue) and RCP8.5 (red). **b**] changes in methane emission estimates between 2000 and 2100 for RCP4.5 and RCP8.5. Spread, denoting climate uncertainty, is shown by light blue (RCP4.5) and pink (RCP8.5) box and whiskers. **c**] linearised estimates of changes to methane emissions from 2000 to 2100 under RCP4.5 and RCP8.5²⁵² owing to inundation extent soil temperature NPP and inundation extent + soil temperature + NPP. In all cases, boxes describe the interquartile range (IQR), the whiskers the quartiles $\pm 1.5 \times$ IQR, circles outliers, and the orange and dashed black lines the mean and median values, respectively, associated with the ensemble of model runs. Future increases in methane emissions are driven equally by warmer temperature, higher rainfall and larger NPP. The solid horizontal lines in b and c denote the zero line.

1659 **Supplementary Information** << new file >>
1660

1661 To understand the response of wetland methane emissions over Eastern Africa to future
1662 climate output from the JULES land surface model^{253,254} is analysed, coupled with the
1663 IMOGEN impacts model^{252,255}. IMOGEN is calibrated against 34 different CMIP5 ESM-based
1664 climate simulations where the climate is described using pattern-scaling²⁵⁶.

1665
1666 Fitted to the climate projection from each ESM, IMOGEN assumes a linear relationship at
1667 each grid-box and for each month between changes in meteorology and global warming, itself
1668 a function of atmospheric radiative forcing. The IMOGEN system allows an exploration of the
1669 uncertainty in the climate projections and the wetland methane emission models. The JULES
1670 wetland methane emissions model is driven by wetland extent, available substrate, and soil
1671 temperature.

1672
1673 In this analysis net primary productivity as a surrogate for the substrate²⁵². Ranges of regional
1674 totals are used to described wetland model uncertainty, based on the best current global
1675 totals²⁵² and a range of temperature sensitivities²⁵².
1676